A Review on Gain Enhancement Techniques for Vertically Polarized Mid-Air Collision Avoidance Antenna for Airborne Applications

M. PALLAVI [1,2], **(Graduate Student Member, IEEE), PRAMOD KUMAR**[1],
TANWEER ALI[1], **(Senior Member, IEEE), AND SATISH B. SHENOY**[2,3]
[1]Department of Electronics and Communication Engineering, Manipal Institute of Technology, Manipal Academy of Higher Education, Manipal 576104, India
[2]Centre of Excellence in Avionics and Navigation, Manipal Academy of Higher Education, Manipal 576104, India
[3]Department of Aeronautical and Automobile Engineering, Manipal Institute of Technology, Manipal Academy of Higher Education, Manipal 576104, India

Corresponding authors: Tanweer Ali (tanweer.ali@manipal.edu) and Pramod Kumar (p.kumar@manipal.edu)

ABSTRACT Mid-air collisions (MACs) are commonly caused by temporary or permanent loss of flight control resulting in catastrophic damages and hence must be countered with suitable technology. The avionic industry has been using Traffic Alert and Collision Avoidance System (TCAS) for avoiding mid-air collisions since 1987. The TCAS either uses an Omni-directional antenna or a directional antenna for the surveillance of other nearby aircraft. The existing TCAS directional antennas, i.e., an array of monopole antennas are characterized by a maximum gain of 3.6 dB, which is regarded as low. As a result, many research has been carried out to find the alternative for the TCAS antenna and have found microstrip patch antenna (MPA) which yield some promising results such as feed flexibility, multiband, beam steering, etc. However, the MPA still suffers from disadvantages such as low gain and narrow bandwidth. Hence, lately, a tremendous amount of work has been carried out to enhance the gain of the MPA. In this paper, we first review the key methods that has been reported so far to improve the gain of the traditional TCAS antenna. We note that, in most of the reported work, conventional techniques such as parasitic patches, and shorting pins are used to improve the gain of MPA, and no substantial work was done using advanced techniques such as electromagnetic-band gap (EBG), metamaterials and metasurfaces. Hence, we further review the work that has been carried out to improve the gain of vertically polarized MPAs using advanced techniques for L- and S-band (up to 3 GHz). Many advanced structures that are easily adapted to enhance the gain of TCAS antenna are thoroughly discussed in this work.

INDEX TERMS Array, electromagnetic-band gap, metamaterials, metasurface, parasitic patch, shorting pins, superstrate.

I. INTRODUCTION

The Traffic Alert and Collision Avoidance System/ Airborne Collision Avoidance System (TCAS / ACAS) is the outcome of more than 30 years of extensive research by the Federal Aviation Administration (FAA), the Civil Aviation Authorities (CAAs), and the Aerospace Industry. This system has been developed to minimize mid-air collisions or air accidents between aircraft [1], [2]. The basic functional diagram of the TCAS is illustrated in Figure 1, and it is composed of Traffic Advisory (TA) & Resolution Advisory (RA) Display, a Control Panel, a TCAS Computer, a Mode S transpon-

The associate editor coordinating the review of this manuscript and approving it for publication was Rosario Pecora.

der, Aural Annunciator, and antennas. The TCAS directional antenna is mounted on the top of the airline to monitor any nearby aircraft and, if there is any threat, it alerts the pilot by sending the range and altitude information of the other aircraft via cockpit displays and alarms. Generally, this antenna transmits the radio signal at a constant rate that is per second at 1.09GHz to detect any nearby aircraft, and the TCAS receiver antenna, which operates at 1.03GHz, gathers the reply data from nearby aircraft and sends it to the TCAS as shown in Figure 2.

Presently, an array of four monopole stubs are used as a TCAS directional antenna, and it is mounted above the aircraft. The specifications of the existing TCAS directional antenna are summarized in TABLE 1. From references listed
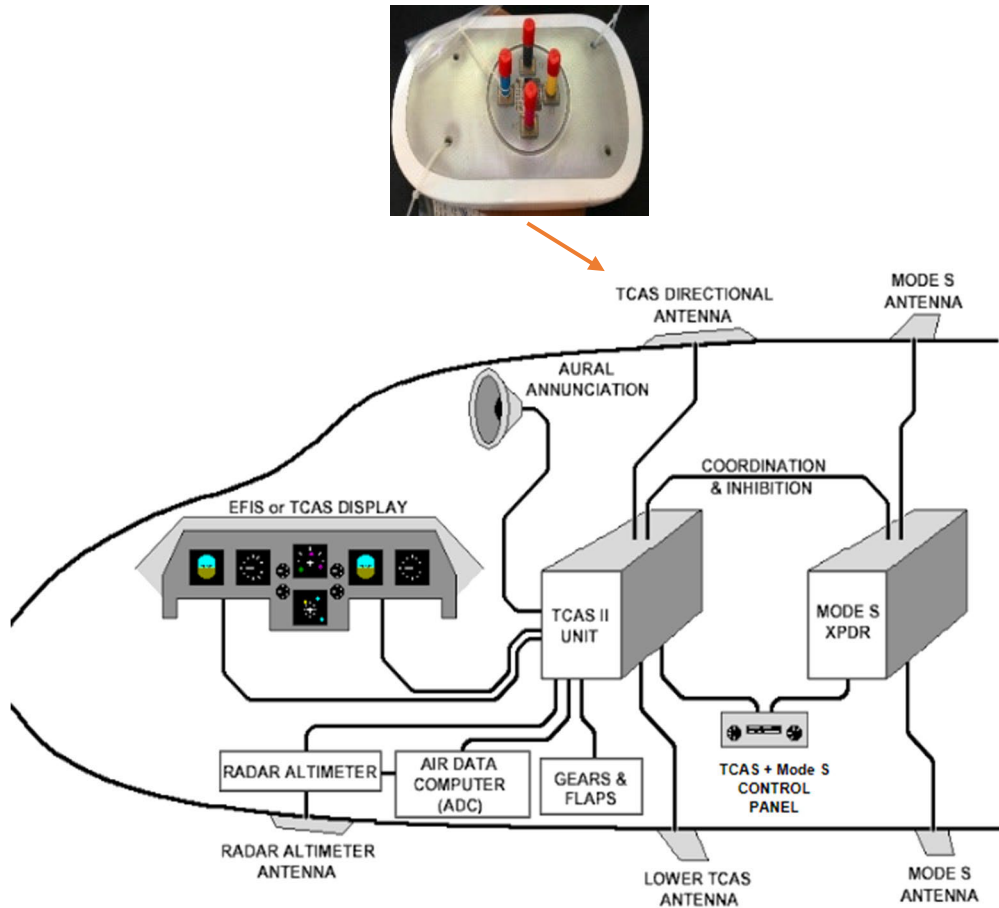
in TABLE 1, we note that the conventional TCAS antenna is inherently affected by the low gain (3.6 dB), high side-lobe level (-8dB), wide-beam width ($>100^0$), tuning, and scanning issues related to both beam and frequency.

The low gain of the TCAS antenna signifies that the power dissipation during signal transmission is very high whereas, the high side-lobe level (SLL) reduces the coverage distance of the antenna, and if the coverage distance decreases, then the number of flights detected in the surrounding airspace decreases, which are likely to pose a significant threat of collision.

The size and structure of the TCAS directional antennas are primarily restricted to aircraft dimensions (such as physical length, width, and height) and aircraft operations (such as military or commercial aircraft), and these antennas are exposed to very harsh environments, thus avionics applications prefer low profile, electrically small size, flexible, and highly robust antennas. The radiation characteristics of the monopole antenna are primarily dependent on the ground plane. In avionics, the skin of the aircraft will act as a ground plane for the antennas, and since many systems have to be mounted on the top of the aircraft, very limited space will be allocated to the antenna which restricts the ground plane. The

TABLE 1. Characteristics of traditional TCAS antenna [5].

Characteristics	Values
Transmitting Frequency	1.03 GHz
Receiving Frequency	1.09 GHz
V.S.W.R	1-1.5
Impedance	50 Ω
Power	1000 Watt/Peak
	Polarization: Linear
Directional Antenna	Gain: 3.6 dB
	Side-Lobe: -8 dB
	Beam width: More than 100^0
Omni-directional Antenna	Gain: 1 dB

curved surface, the asymmetric shape of the aircraft platform, and the compact size of the antenna ground plane will have a significant effect on the overall performance of the antenna.

In recent years, combinations of different composite materials have been used to build aircraft body instead of aluminium. These composite materials will increase rigidity, mitigate corrosion, and greatly reduce the overall weight of the aircraft. As the aircraft surface functions as a ground plane to the monopole antenna, the conductivity of the composite materials will further degrade the performance of the
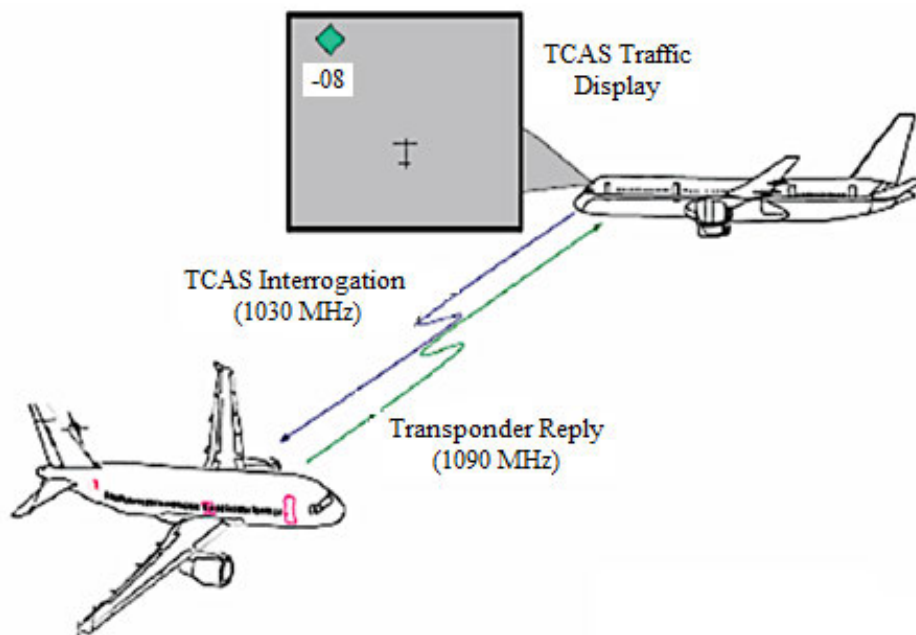
FIGURE 2. Basic operation of TCAS/ACAS [4].

antenna (especially gain). Many research [6]–[8] has been conducted to investigate the impact of a restricted ground plane on the overall performance of the antenna and how this antenna is not a very good option for airborne applications. In 1997, Johnson and Rahmat-Samii developed a printed monopole antenna for airborne applications, and several research studies have been undertaken over the years to find appropriate printed monopole antennas [9], [10] for aircraft. In [11]–[13], the previous work on printed monopole antennas for aircraft applications has been reviewed and it has been reported that the printed monopole antenna is not a good choice for airborne applications due to its larger size which is ∼0.3λ (where λ is free space wavelength at lower operating frequency). Since the required antenna for the TCAS application needs to be compact, low profile, robust, flexible, easily mounted at the different locations on the skin of the aircraft, the best choice is to replace the monopole antenna with a microstrip patch antenna (MPA). In contrast to any conventional antennas, MPA is rapidly developing and commonly used in most applications because of its advantages like low profile, lightweight, low cost, and ease of fabrication [14]. The MPA is well suited to airborne applications due to its characteristics such as feed flexibility, multiband, beam steering, different polarization, beam shaping, and robustness when mounted on any rigid surface [15]. Although it provides so many desirable features, it still suffers from a few inherent disadvantages, such as low radiation efficiency, low gain, and narrow operating bandwidth.

There are three types of losses that are responsible for the performance degradation of the MPA, namely dielectric loss, conductor loss, and surface wave loss. The conductor

and dielectric losses depend primarily on the quality and loss tangent of the material being used to construct the patch and the substrate, while the surface wave loss relies mainly on the substrate thickness and the permittivity of the materials. Because of these losses, the maximum achievable gain from the unit element MPA is limited to 5-9 dB [16]. Since the gain of the MPA is relatively poor, it has been restricted from a wide range of applications, so a lot of efforts have been made to enhance the gain of the conventional MPA.

The location allotted to place the TCAS antenna on the aircraft body is fixed which is above the second window on the front side of the aircraft [17], [18]. When the TCAS antenna is vertically polarized, it has reported better mutual coupling, lower mean, maximum standard deviation, and very good variance value. In recent years, several circularly polarized (CP) MPAs have proposed to increase the gain at the low-frequency band (up to 3 GHz) [19], [20]. The CP antennas have good signal propagation characteristics, strong mutual coupling, higher directive gain, reasonable side-lobe level, and good beam efficiency [21] and are commonly used for GPS applications [22], satellite communication [23], pulse compression radar [24], and BeiDou navigation systems [25] and so on. The TCAS antenna with circular polarization has never been practically tested due to lack of complete radar coherence matrix of phase and amplitude, and inadequate information on whether the signal level of the circularly polarized channel remains always high to make it work for this particular application [26]–[29]. Since all the previous work on TCAS antenna designing has considered vertical polarization, in this review paper, we have reviewed only vertically polarized MPAs.
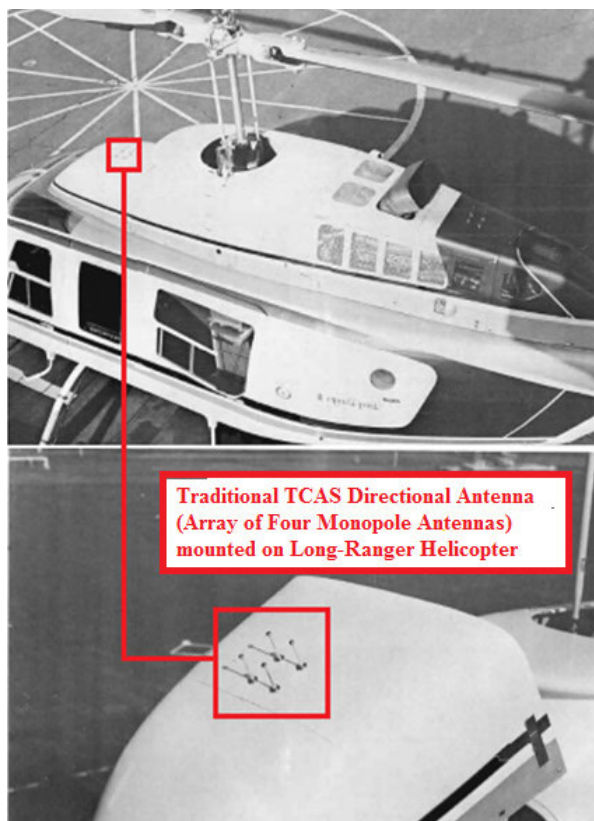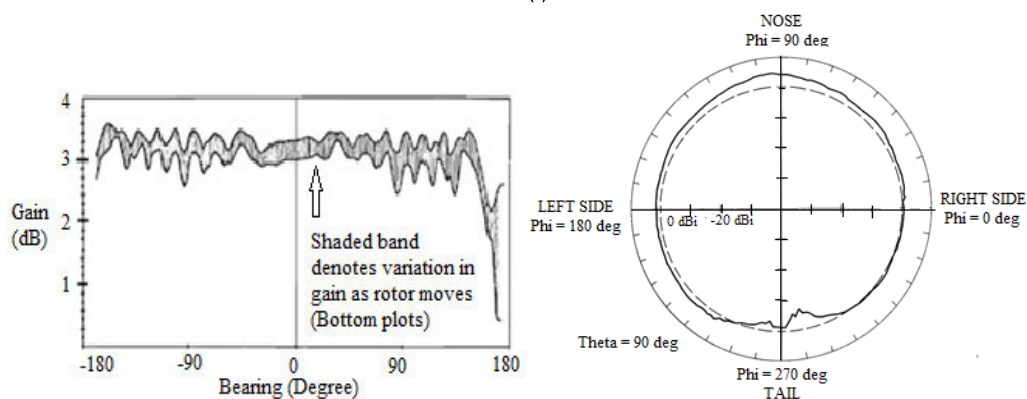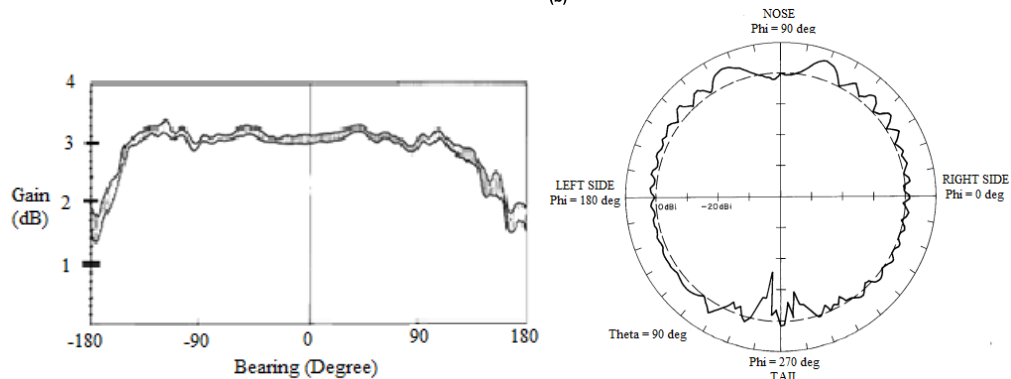
FIGURE 3. Traditional TCAS directional antenna (a) mounted on long-ranger helicopter (b) gain vs. bearing angle plot and radiation pattern plot for directional antenna with Helicopter Shaft (c) gain vs. bearing angle plot and radiation pattern plot for directional antenna with helicopter shaft and absorbing material [30].
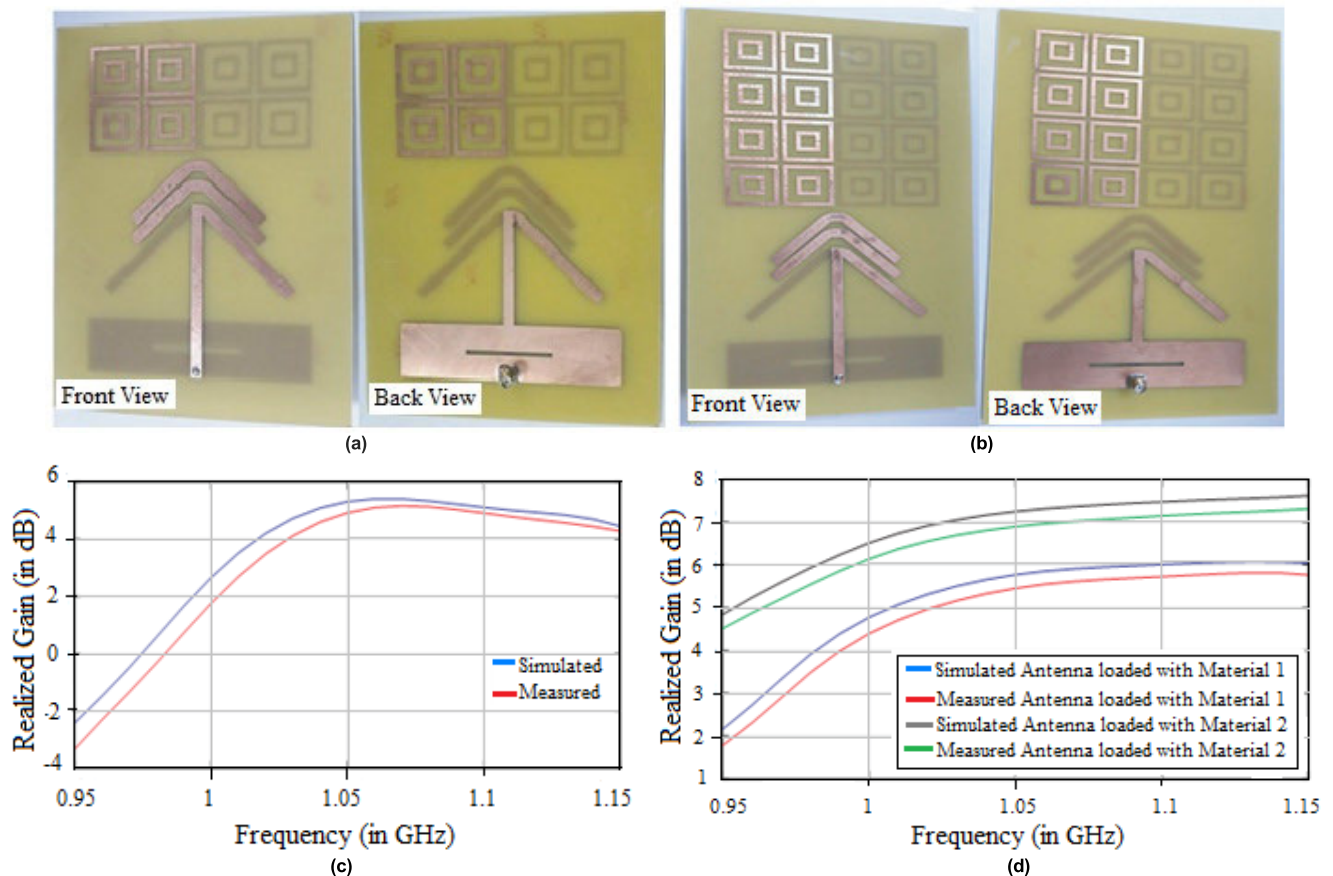
FIGURE 4. Folded dipole antenna structure (a) with 2 × 4 SRR structure (b) with 4 × 4 SRR structure (c) gain plot of folded dipole antenna without SRR structure (d) gain plot of folded dipole antenna with 2 × 4 and 4 × 4 SRR structure [32].
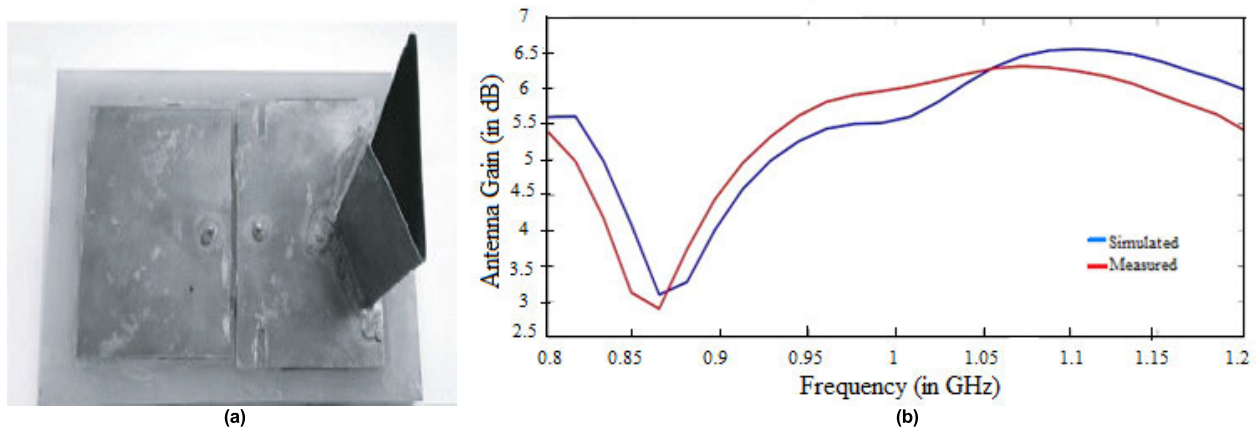

FIGURE 5. Fabricated prototype of the TCAS directional antenna (a) a unit-element MPA (b) gain vs. frequency plot [31].

In this paper, the work done so far to improve the gain of a TCAS directional antenna using MPA is initially reviewed. Next, the wide range of work done to improve the gain of MPA particularly for L and S-band (up to 3 GHz) using many conventional and advanced techniques is discussed. This paper has discussed many advanced structures, which are loaded on the patch, on the ground plane, used as a substrate, and as a superstrate to enhance the gain of the MPA. The main motive of the review work is to provide key aspects for researchers working on the design of a high-gain MPA for TCAS applications, outlining the advantages and disadvantages of each method, making it much easier to choose the best techniques for this application.
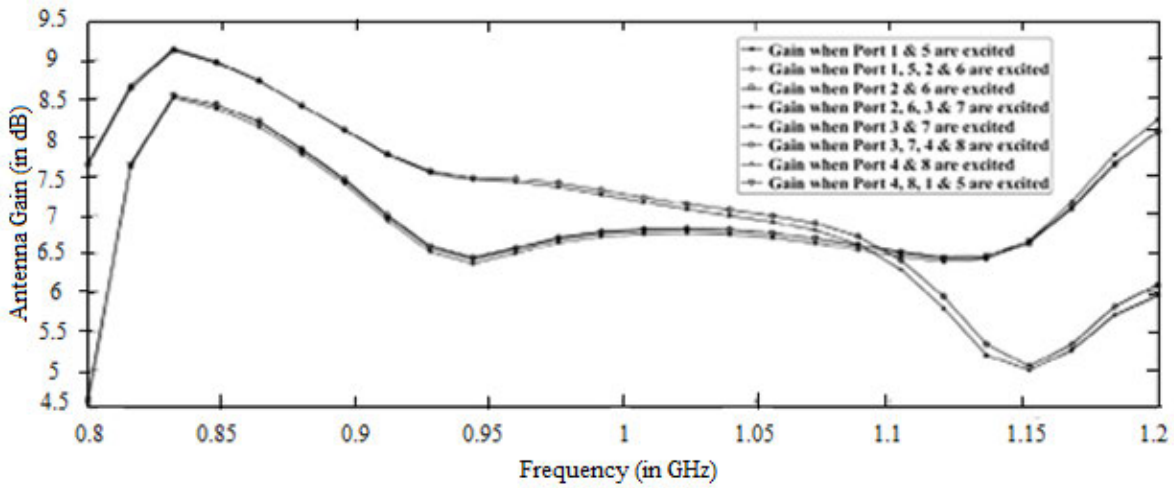
II. CONTRIBUTION

The key contribution of this article is as follows:

- It provides an overview of all related work on the TCAS antenna, a variety of different methods to mitigate the disadvantages of the conventional TCAS antenna.

(a)

(b)

(a) Port 1 & 5   (b) Port 1, 5, 2 & 6   (c) Port 2 & 6   (d) Port 2, 6, 3 & 7

(e) Port 3 & 7   (f) Port 3, 7, 4 & 8   (g) Port 4 & 8   (h) Port 4, 8, 1 & 5
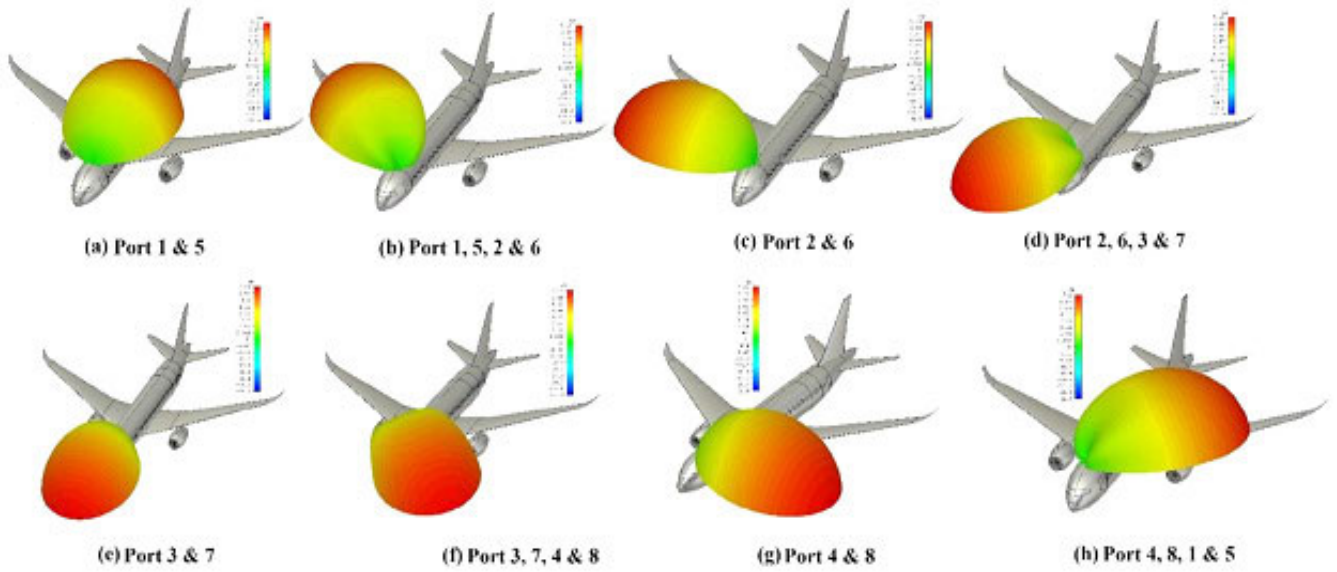
(c)

FIGURE 6. Fabricated prototype of the TCAS directional antenna (a) quad-element MPA (b) gain vs. frequency plot for different port combination (c) antenna structure mounted on CAD model of aircraft to analyse the change in gain [33].

- The article also addresses the current challenge of achieving high gain, low side-lobe level, narrow beam width, compact size, and vertically polarized directional antenna.
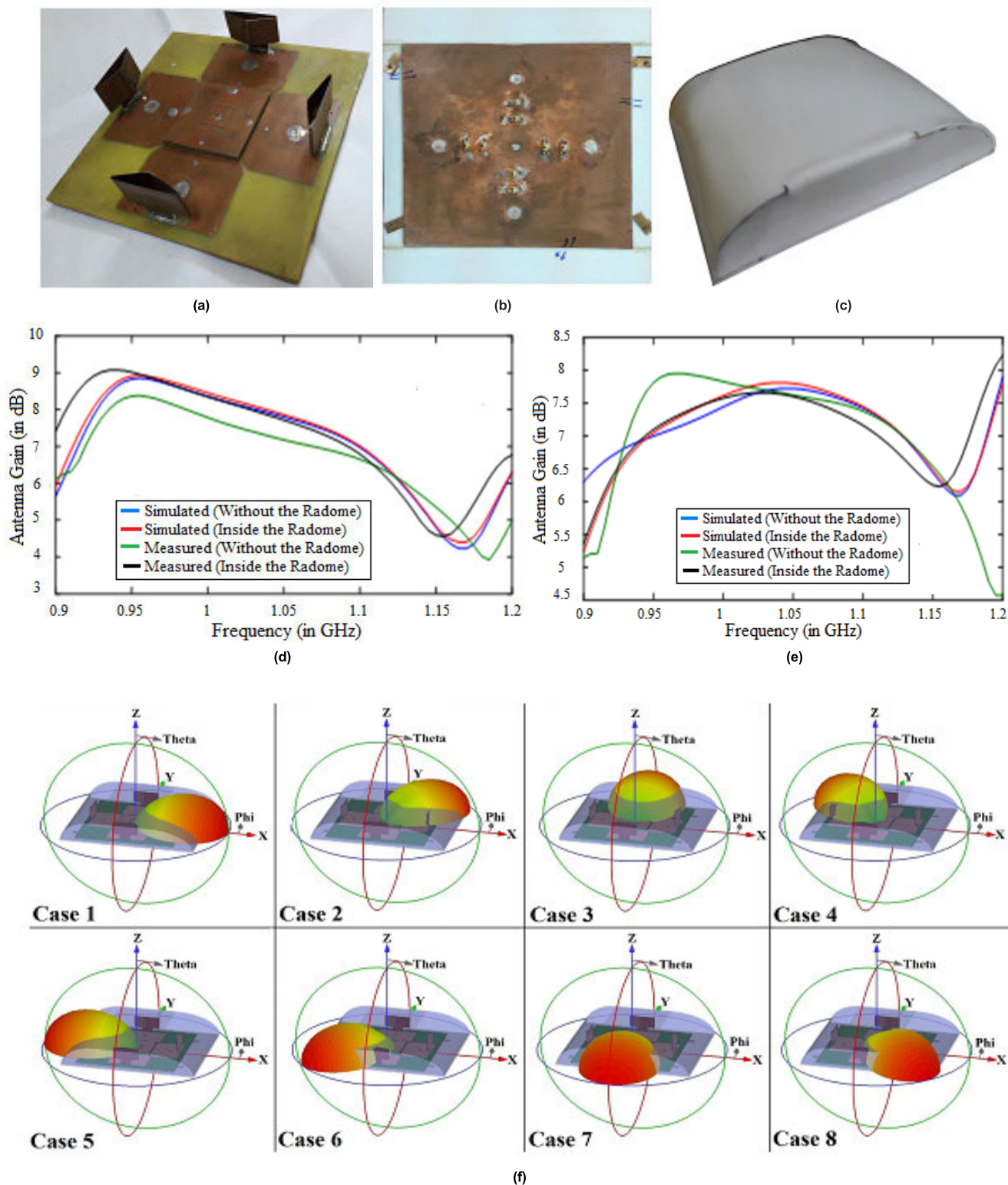
FIGURE 7. The Quad-element MPA structure with radome (a) antenna structure placed inside the radome (b) bottom view of the antenna inside the radome (c) the antenna structure encapsulated inside the aerodynamic shaped radome structure (d) gain plot of the proposed antenna inside the radome for case 1,3,5, and 7 (+0⁰, +90⁰, ±180⁰, and −90⁰) (e) gain plot of the proposed antenna inside the radome for case 2,4,6, and 8 (+45⁰, +135⁰, −135⁰, and −45⁰) (f) 3D radiation pattern for different ports [34].

- Many advanced structures such as EBG, Metamaterials, and Metasurface, which are the future choices for enhancing the overall performance of the TCAS antenna, are discussed in detail.

FIGURE 8. The proposed antenna structure for TCAS application (a) schematic structure (b) parasitic element (c) antenna structure and the transformer network (d) gain plot in the directional mode (e) gain plot in the Omni-directional mode [35].
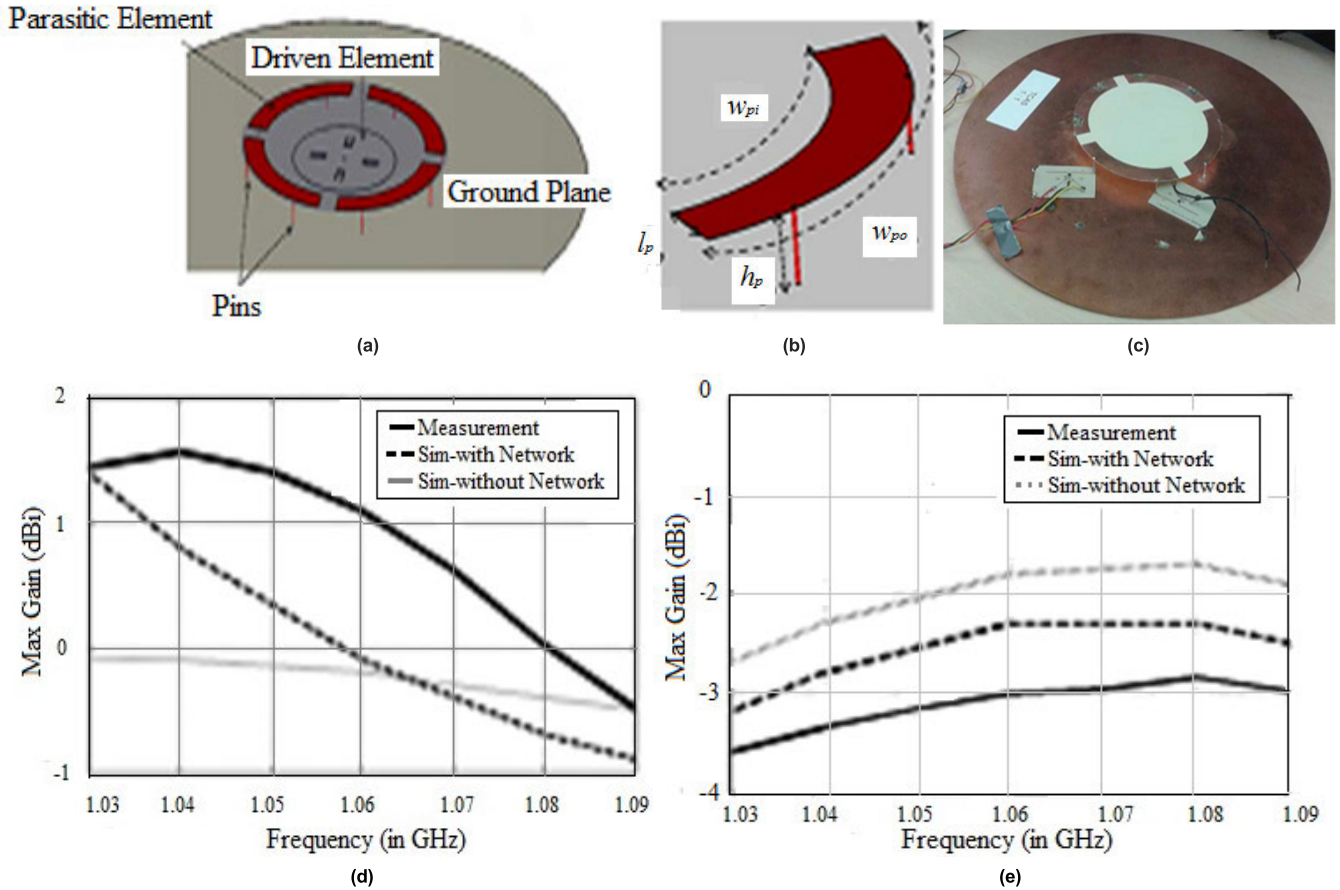
- The advantages and challenges of many structures on both conventional and advanced gain enhancement techniques are addressed with a lot of references to provide a better understanding for researchers working on the design of the TCAS antenna.

The rest of the paper is arranged as follows. In Section III, we briefly discuss previous works on the TCAS directional antenna. In section IV, the conventional and advanced gain enhancement techniques for the MPA that are appropriate for TCAS applications are reviewed. In section V, both conventional and advanced gain enhancement techniques and their impact on the overall performance of the antenna are discussed. Lastly, Section VI presents a few general observations and conclusions of the study.

III. RELATED WORK ON TCAS DIRECTIONAL ANTENNA

In this section, we discuss the work carried out so far to enhance the TCAS directional antenna gain. The traditional TCAS directional antenna which is mounted on top of the Long-Ranger Helicopter [30] is illustrated in Figure 3(a). The gain variance of the antenna with and without absorbing material was shown in Figure 3(b) & (c), respectively, and a maximum gain of 3.6 dB was recorded in this work.

The overall characteristics of this antenna are summarized in TABLE 1.

The addition of the 2×4 SRR structure increased the gain by 1.07 dB and 0.7 dB, and the 4×4 SSR structure improved the gain by 2.6 dB and 2.1 dB at 1.03 GHz and 1.09 GHz, respectively. In [31], TCAS directional antenna is designed using a patch antenna, and to improve the gain of the MPA two shorting pins were used and this design has improved the gain by 2.86 dB which is illustrated in Figure 5(b).

To enhance the gain of the TCAS directional antenna, a circular array of patch antenna has been proposed in [33], the use of eight shorting pins has improved the gain by 3.8 dB which is illustrated in Figure 6(b). In this work, the proposed MPA was mounted on the CAD model of Boeing 787, as shown in Figure 6(c), to test the gain improvement by sequentially switching the combination of eight different ports. To shield the proposed antenna from bad environmental conditions during flight, an aerodynamically shaped radome is designed in [34]. The effect of the radome on the overall performance of the TCAS antenna was extensively studied by sequentially exciting different ports (eight ports) as shown in Figure 7(d), and it was observed that the proposed antenna with radome has further increased the gain by 0.5 dB and 0.7 dB at 1.03 GHz and 1.09 GHz, respectively.
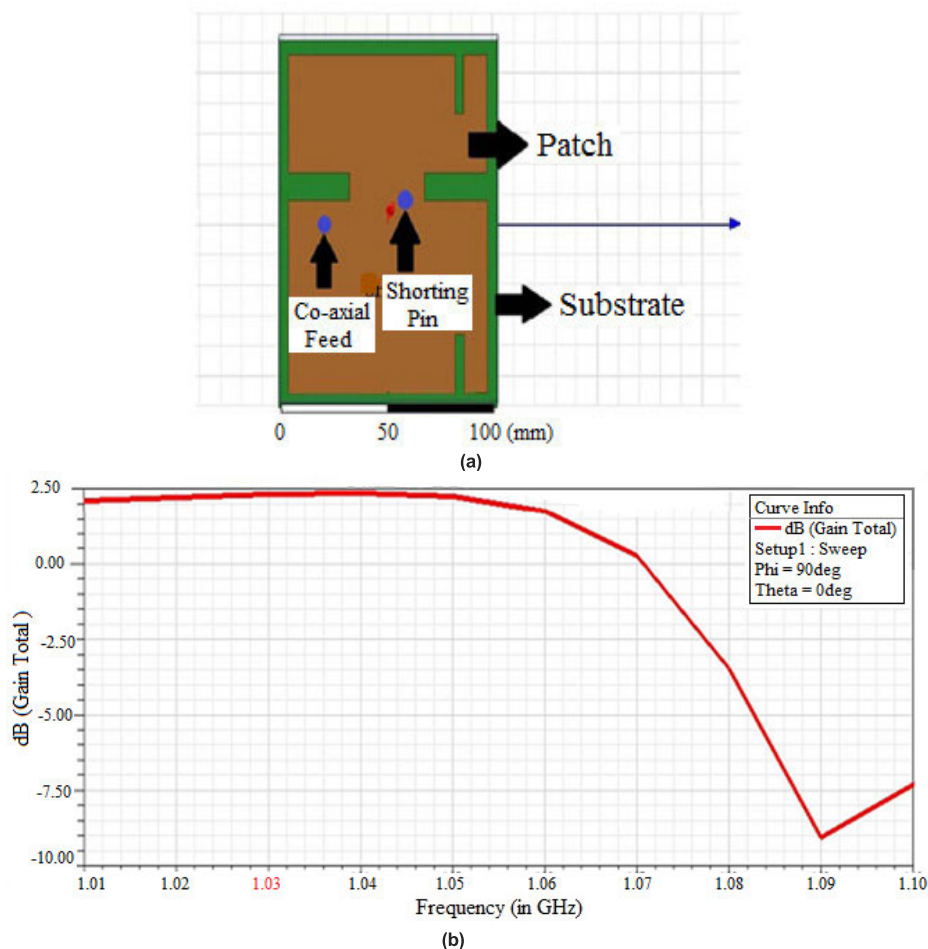
FIGURE 9. Unit-element MPA for TCAS application (a) schematic structure (b) gain vs. Frequency plot [36].

A printed monopole antenna with parasitic patches and shorting pins was proposed in [35]. Here the performance of the antenna (especially the gain) was adversely affected by the use of the transformer circuit for the beam switching operation as shown in Figure 8 (d) & (e).

A slotted rectangular MPA with a shorting pin aiming to reduce the size of the TCAS antenna was proposed in [36], the maximum gain obtained by this method is 2.47 dBi, which is 1.1 dBi lower than the traditional TCAS antenna as illustrated in Figure 9(b). The primary goal of the work is to reduce the size of the TCAS antenna. A coaxial-fed circular microstrip patch antenna was proposed in [37], two slots were etched on the proposed design to provide the dual resonance, and a shorting pin was used to improve the gain. As shown in Figure 10 (c), the maximum gain obtained by this approach was 6.59 dB, which is 2.99 dB higher than the traditional TCAS antenna. In [34], the etching of eight identical shortening pins on the patch increased the TCAS antenna gain by 4.5 dB, which was recorded as a significant improvement. The most relevant existing work on the TCAS directional antenna is summarized in TABLE 2. It is observed that, in most of these works, conventional methods such as

parasitic patch and shorting pins are used to improve the patch antenna gain.

IV. GAIN ENHANCEMENT TECHNIQUES FOR MICROSTRIP PATCH ANTENNA

So far, many distinctive methods have been reported to increase the gain of the MPA. In this section, several gain enhancement techniques proposed for low-band (up to 3GHz) MPA is discussed by dividing them into two groups, namely conventional/traditional techniques and advanced techniques. The various gain enhancement techniques covered in this article have been outlined in Figure 11.

A. CONVENTIONAL/TRADITIONAL TECHNIQUES

The very basic or conventional methods available to enhance the gain of the MPA are; the concept of an array, the coupling of the parasitic patches, and the loading of the shorting pins. The array technique is the most promising method to improve the gain of any antenna, but in TCAS applications, because the size allocated to the directional antenna is fixed, the array method is not much preferred. The antenna elements are arranged circularly to cover the maximum
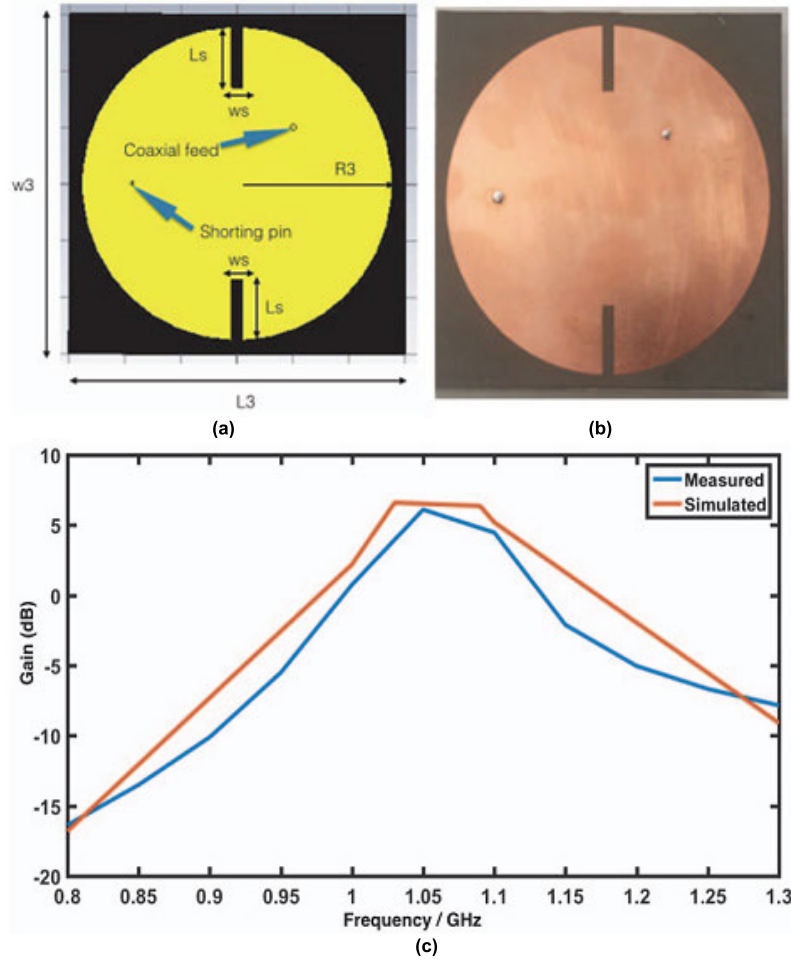
FIGURE 10. The unit-element circular MPA for TCAS application (a) schematic structure (b) fabricated prototype of the proposed antenna (c) gain vs. frequency plot [37].

TABLE 2. Summary of research on TCAS directional antenna.

Ref	Dimension (mm³)	Dielectric substrate	Gain enhancement (dB)	Gain enhancement technique	Shape of elements	No. of elements	Freq. band
[30]	224 x 224 x 4	Rogers RT/ Duroid 5880, εr = 2.2, tanδ = 0.0009	--	--	Circular	4	
[31]	157 x 110 x 1.6	FR4, εr = 4.4,tanδ = 0.02	2 (at 1.03Hz) & 3 (1.09 GHz)	Shorting pins	Circular	2	
[32]	130 x 118 x 1.6	FR4, εr = 4.4,tanδ = 0.02	3.2 (at 1.03Hz) & 3.6 (1.09 GHz)	SRR	Square	4 x 4	
[33]	224 x 224 x 4	FR4, εr = 4.4,tanδ = 0.02	3.8 (at 1.03Hz) & 3.3 (1.09 GHz)	Shorting pins	Circular	8	*L - B A N D*
[34]	224 x 224 x 4	FR4, εr = 4.4,tanδ = 0.02	4.5 (at 1.03Hz) & 4.2 (1.09 GHz)	Shorting pins	Circular	8	
[35]	D = 170, h = 17	Rogers 6010, εr = 10.2	1.5	Shorting pins & Parasitic patches	Vertical line & Concentric Circle	4 & 4	
[36]	100 x 150 x 3	Rogers RT/ Duroid 5880, εr = 2.2, tanδ = 0.0009	1.1	Shorting pin	Circular	1	
[37]	120 x 120 x 3.18	Rogers RT/ Duroid 5880, εr = 2.2, tanδ = 0.0009	3.09 (at 1.03Hz) & 2.86 (1.09 GHz)	Shorting pins	Circular	2	

region and not to improve the gain. Hence, the array technique for gain enhancement has not been reviewed in this work.

1) PARASITIC PATCH

The parasitic element or passive radiator is a conductive element that is not directly connected to the feed but is located
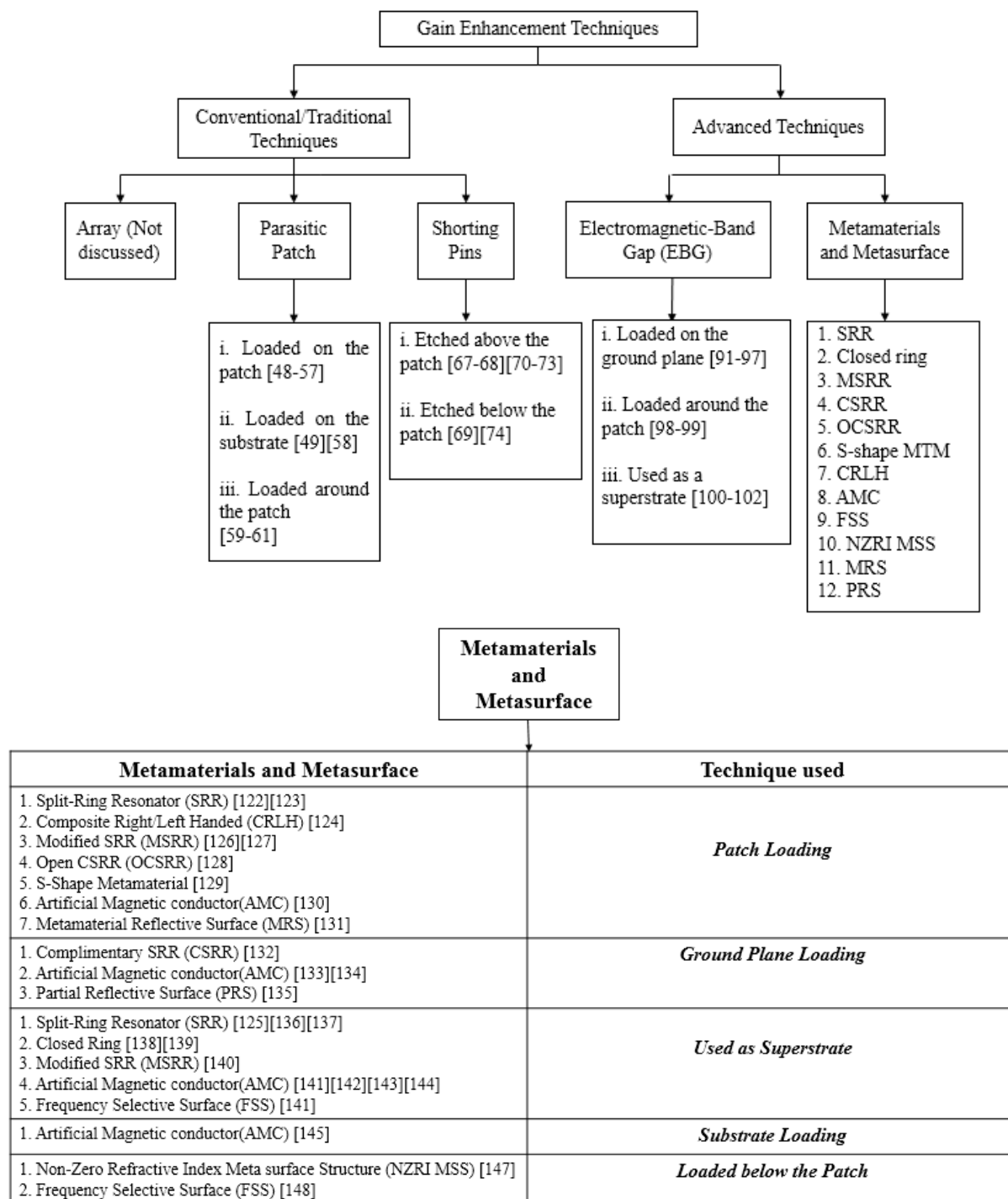
FIGURE 11. The flow diagram of various gain enhancement techniques.

close to the main radiator or patch antenna [38] as illustrated in Figure 12.

In this method, stacked or planar configuration parasitic patches are electromagnetically coupled with the primary patch [40], [41]. When the stacked parasitic patch is located approximately half a wavelength away from the primary patch, a significant gain increase has been reported in [42], [43]. It has also been validated in [44], [45] that the gain improvement is very significant when the separation between the parasitic patch and the fed patch is around 0.3 to 0.5λ. Although it has a single radiator element that is a primary patch, due to the inclusion of parasitic elements, it functions much like an array antenna.

FIGURE 12. Parasitic patches around the driven patch [39].

Several pioneering works [15], [46]–[49] has shown that, based on the separation 's' between the primary patch and the parasitic elements, the characteristic plot of the EM-coupled antenna would be divided into three regions as illustrated in Figure 13, 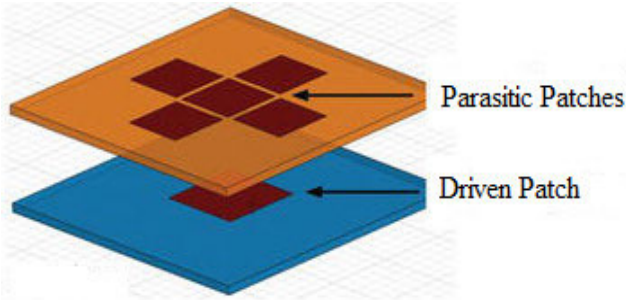in the first region a good bandwidth improvement is possible, the second region is not optimal for antenna applications due to poor radiation characteristics, and in the third region significant gain improvement with 1% bandwidth enhancement is possible. Figure 14 [50] shows the TCAS directional antenna with parasitic patches that are placed on the aircraft.

In an array technique, each element will be directly connected to the feed line, due to which the feeding network would introduce copper losses and unwanted radiations, and each element requires a phase shifter that increases the complexity and expense of the antenna [51]. To reduce the limitations stated above, the main array is dissected into sub-arrays, and each sub-array consisting of only one fed or driven patch element with several closed parasitic elements located around the patch and derives its energy from the near-field coupling to the driven patch [52]. Parasitic elements control the trajectory of the antenna beam without narrowing the beam, and by adjusting the position, length, width, and the number of parasitic patches, the direction of the radiation beam can be adjusted as needed [53], [54].

In a miniaturized antenna, the overall size of the antenna is greatly reduced and the width of the antenna has been made very narrow. Hence, it results in a large current and consequently large I^2R loss, especially at the edge of the patch antenna [55]–[59]. This is the main reason behind the drastic decline in gain and efficiency of the antenna. To increase these parameters of the miniaturized patch antenna, a new technique is introduced in which the traditional single conductor layer of the antenna is replaced by multiple, thin laminated conductor or stacked layers as illustrated in Figure 15. These multiple layers increase the depth of penetration of the EM wave, which significantly reduces the attenuation and ohmic losses. Let us assume an antenna design with 'n' number of alternate laminating dielectric and conducting layers as shown in Figure 15 (b).

The electric and magnetic field equations for the nth layer is given by [60],

$$E_{2n} = C_{2n} \exp\left(-jk_m z\right) + C_{2n+1} \exp\left(jk_m z\right) \tag{1}$$

$$H_{2n} = \frac{k_m}{\omega \mu_m} C_{2n} \exp\left(-jk_m z\right) - \frac{k_m}{\omega \mu_m} C_{2n+1} \exp\left(jk_m z\right) \tag{2}$$

The power dissipation in the considered n-layer antenna is calculated using the following equation:

$$P_L = \frac{1}{2\eta} - \frac{|C_1|^2}{2\eta} - \frac{|C_{2n+2}|^2}{2\eta} \tag{3}$$

where, C_1 amplitude of the reflected waves, C_{2n+2}; amplitude of the transmitted waves.

The MATLAB tool is used to solve the aforementioned equation and to find the power dissipation of the antenna with conductivity $\sigma m = 10^5$. Figure 15 (c) illustrates that the ohmic loss decreases significantly when a single layer is superseded by several thin conducting layers. It is observed from the graph that the ohmic loss reduction is very high when the number of layers is between 2 and 5 when the layer is between 5 and 15 the loss reduction is moderate, and for 25 layers the power loss is not significant, but the loss is still less than the single conductive layer. Figure 15(d) shows the difference in the gain for single and multilayered conductors. The overall gain for the single conductor layer is just 1.52 dBi, but the gain for the 3 laminated layers has risen significantly to 2.88 dBi. As shown in Figure 15(e), as the conductive layers increase from one to four, the S11 plot moves to lower frequencies along with the reduction of the S11 value. This is primarily due to impedance mismatch, which could be improved easily by adjusting the capacitive feed line length.

A simple and novel technique is proposed to improve the gain of MPA in [61], where the rectangular loop-shaped parasitic patch is placed on the patch antenna as illustrated in Figure 16, and this method has improved the gain by 3.3 dB (conventional antenna gain is 4.5dB and the proposed antenna gain is 7.8dB).

A stacked MPA with a significantly thick parasitic substrate has been proposed in [62] and the FTDT technique is used to analyze the characteristics of the antenna. Here, the stacked patch characteristics depend on the thickness of the substrate and the separation between the patch and the substrate. If the separation is almost half a wavelength, the standing waves in the gap between two patches would excite and contribute to the radiation, and the leaky resonant cavity would be created between the patch spaces so the interaction of the fed patch cavity would greatly increase the antenna gain. The maximum gain obtained was 10.6 dBi, which is 2.5 dBi higher than the traditional parasitic patch antenna. However, there are few limitations such as difficulty in designing and geometric complexity due to the existence of different radiative / non-radiative patches [63].

The previous research work on the gain enhancement of MPA by the parasitic patch is summarized in TABLE 3.

The work that has been reviewed under the parasitic patch method is for the low-frequency band and the dimension of all selected work is within the assigned size (as specified in TABLE 1) of the TCAS antenna. The maximum gain increase
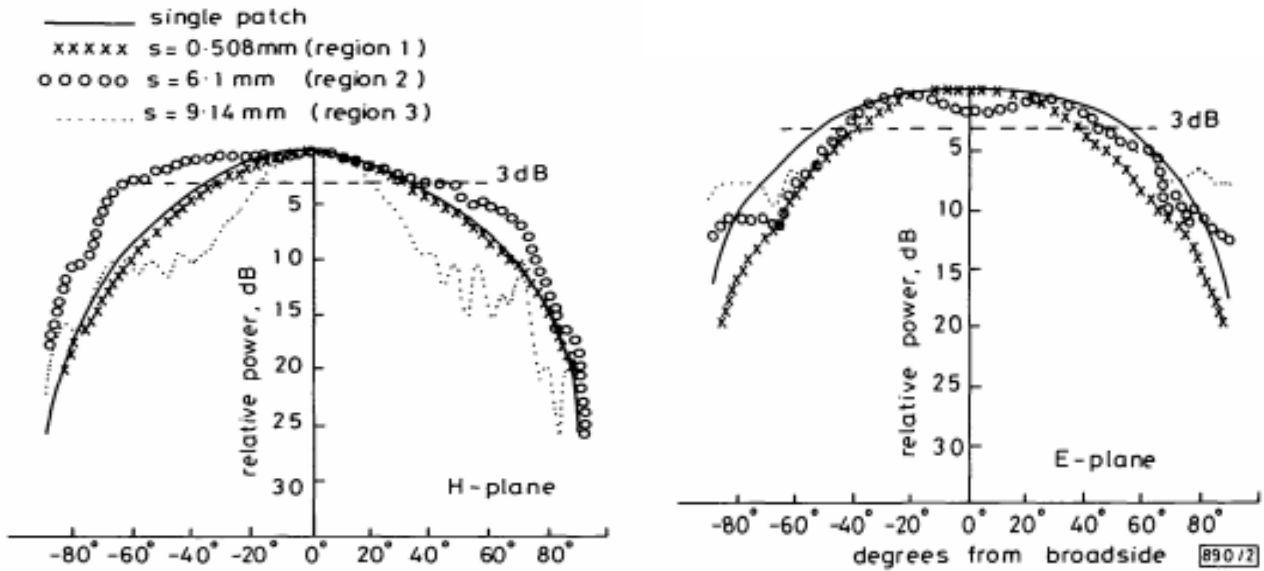
FIGURE 13. Radiation pattern of the electromagnetically coupled rectangular patch antenna with parasitic patch [15].
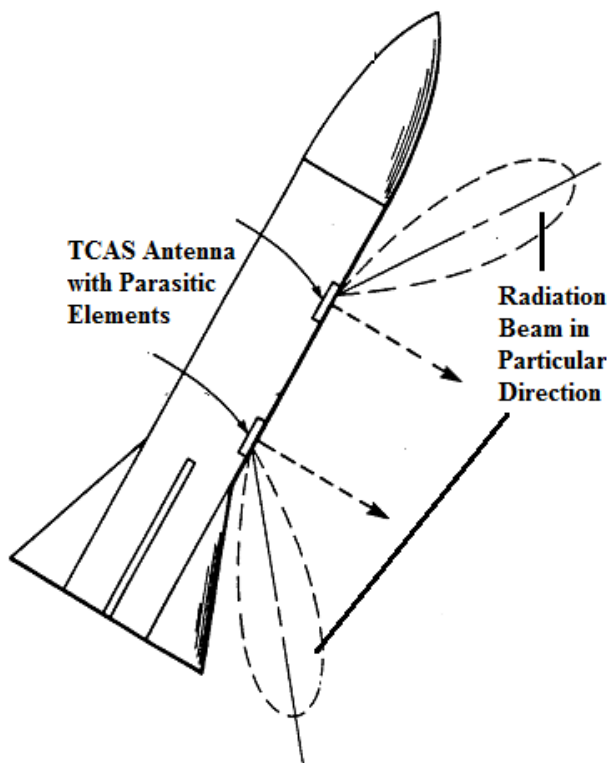

FIGURE 14. TCAS antenna with Parasitic elements mounted on aircraft [50].

using this approach is 3.847 dBi when the parasitic patch is mounted on the main or drive patch.

2) SHORTING PINS

The inclusion of shorting pins increases the geometry of the patch at resonance. The idea of using a pair of shorting pins is to bring an equivalent inductance to the square patch antenna

[44]. The addition of these pins would shift the resonance of the patch to high frequencies, thus increasing the electrical size of the patch antenna, resulting in high gain. The effect of shorting pins on the square patch antenna has been studied in [68] and it has been reported that a large ground plane is required for significant gain improvement due to a fixed number of shorting pins. Theoretically, the addition of more shorting pins to the square patch antenna would significantly shift the resonance frequency, thereby increasing the patch gain.

The behavior of the return loss can be adjusted by diverting the flow of the current of an antenna since the antenna resonance frequency is dependent on the distance traveled by the current. The use of shorting pins will reroute the flow of current from a particular region of the MPA towards the ground plane [75], [76]. However, there is no standard method or equations to find the number and position of the shorting pins to achieve better gain but with reference to many research work, the placing of shorting pins at the center of the patch is considered as the best option [77]. The patch antenna with and without shorting pins and its current distribution has been illustrated in Figure 17 [78]. Here, green color indicates the low current density, yellow denotes moderate current density, and high density is denoted by the red color. In the MPA, the current flow is concentrated primarily on the sides and at the void of the feed point, while the addition of the shorting pins on the MPA would completely alter the current distribution and, here, the current density is maximum at the top center of the patch and moderate at the edges of the antenna [79].

In [80], four identical shorting pins are loaded beneath the single rectangular patch antenna as illustrated in Figure 18 (a) to increase the overall gain. These four shorting pins will significantly disrupt the distribution of the EM field below the patch due to its parallel inductive effect.
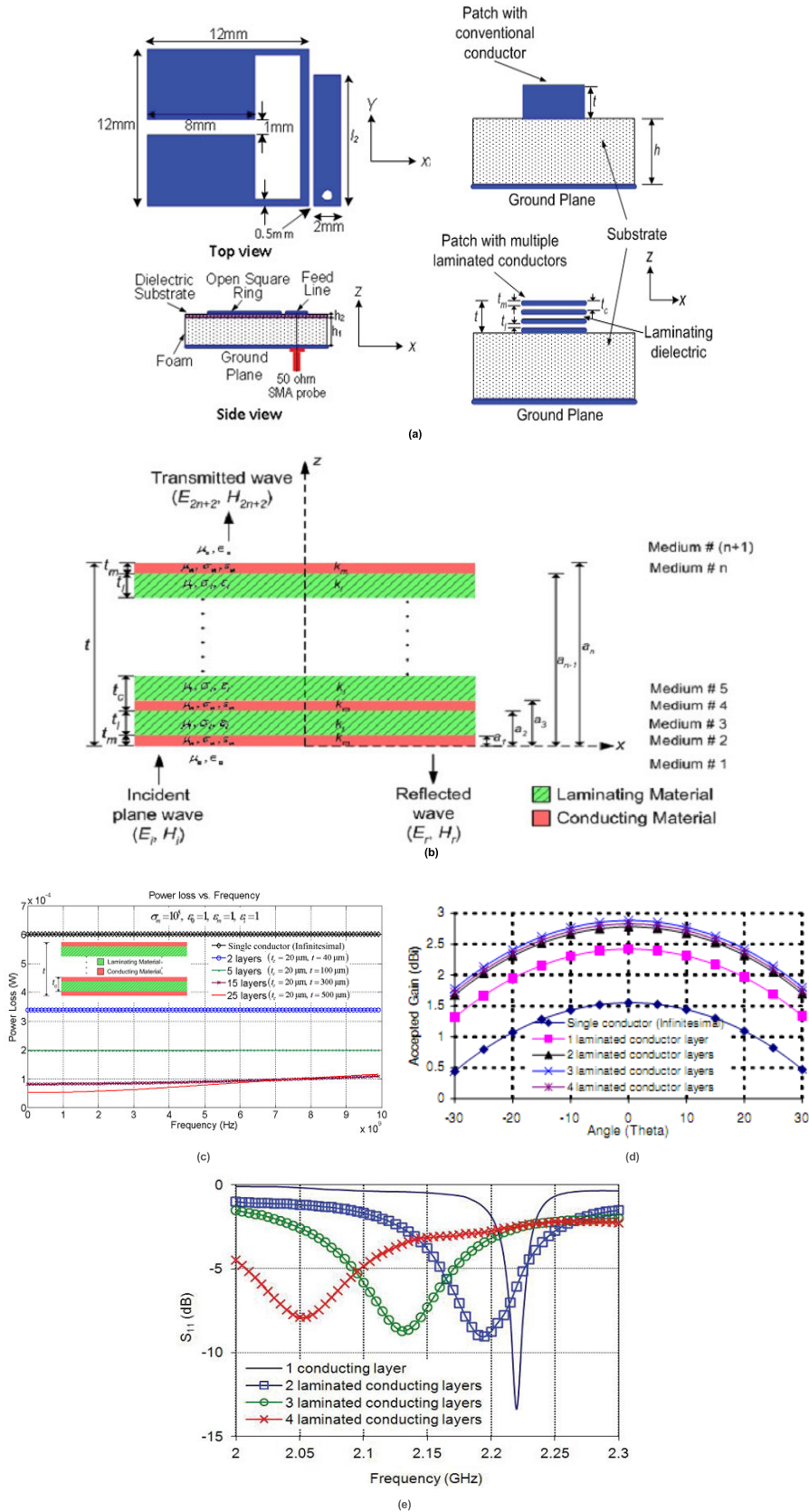
FIGURE 15. Proposed patch antenna (a) geometry of the miniaturized square-ring antenna with single copper conductor and multiple thin laminated conductors (b) the planar material having 'n' number of alternate conducting material and laminating dielectric layers (c) plot of power loss reduction due to multiple thin laminated conductors in contrast to single conducting layer for $\sigma_m = 10^5 \sigma_m = 10^5$ (d) gain variation plot for single and multiple thin layered conductors (e) return loss plot for single and multiple thin layered conductors [60].
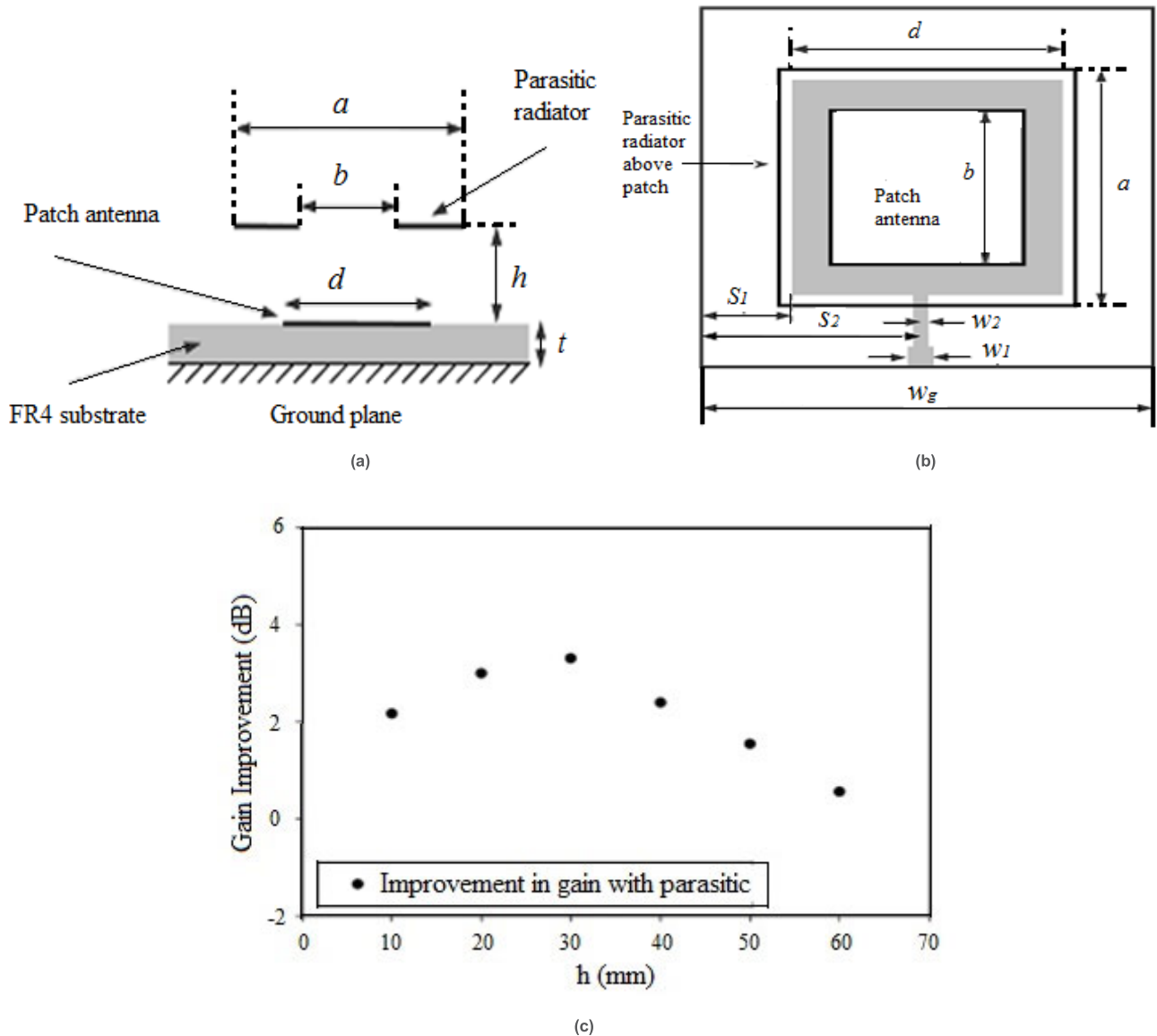
FIGURE 16. Proposed patch antenna with parasitic radiator (a) cross-section of the RMPA with parasitic element (b) top view of the proposed antenna (c) gain vs. thickness of the air (h) [61].

As a result, this inductive effect of the pins increases the total electrical size of the MPA, which in turn increases the radiation area, thereby improving the gain. In comparison to the traditional patch antenna, the addition of shorting pins has increased the gain by 2.9 dBi as shown in Figure 18(b).

As shown in Figure 19(a), a slot and a pair of shorting pins are added to the patch antenna [81]. At first, the slot is etched diagonally from the center of the patch since the central line of the antenna functions as an implicit electric fence having a zero-field effect with the maximum surface current on and below the patch, so the inclusion of the slots in the middle would act as an additional radiator, hence the

radiation produced by this design is similar to three slot array. In addition, two identical shorting pins are positioned longitudinally between the center slots to stabilize the resonant frequency. This method has increased the gain of the MPA by 1.4 dBi, as shown in Figure 19(b).

A number of previous works to improve the gain of MPA using shorting pins are summarized in TABLE 4. All the work that has been reviewed under the shorting pins technique is for the low-frequency band and the dimension of all selected work is within the assigned size of the TCAS antenna. The maximum gain improvement using this approach is 2.9 dBi [82] when four identical shorting pins are placed below the patch and a substantial gain improvement of 2.8 dBi has been

TABLE 3. Summary of research on gain enhancement of MSA using parasitic patch.

Ref	Dimension (mm³)	Dielectric substrate	Gain enhancement (dB)	Gain enhancement technique	Shape of parasitic patch (PP)	No. of parasitic elements	Freq. band
[61]	100 x 120 x 1.6	FR4, εr = 4.4, tanδ = 0.02	3.3	PP on the patch	Square	1	
[62]	36.9 x 36.9 x 0.8	Dielectric, εr = 2.15	2.5	PP on the patch & substrate	Square	2	
[64]	100 x 80 x 10.575	Rogers RT/ Duroid 5880, εr = 2.2, tanδ = 0.0009	1.9	PP on the patch	E shaped	1	
[65]	41 x 37.5 x 1.575	Rogers RT/ Duroid 5870/5880, εr = 2.33	3.847	PP on the patch	Rectangle	1	
[66]	39 x 49.5 x 1.6	FR4, εr = 4.4, tanδ = 0.02	2.61	PP on the patch	Circular	2	*LOW FREQ BAND*
[67]	57 x 77 x 0.76	Dielectric, εr = 2.15	6	PP on the patch	Rectangular	2	*(Up to 3GHz)*
[68]	D= 44mm, H= 1.59mm	FR4, εr = 4.4, tanδ = 0.02	3.8	PP on the patch	Circular	1	
[69]	75 x 75 x 1.6	FR4, εr = 4.4, tanδ = 0.02	3.3	PP on the patch	Triangle	2	
[70]	120 x 120 x 3	FR4, εr = 4.4, tanδ = 0.02	1.58	PP on the patch	Rectangular	4	
[71]	10 x 19 x 0.25	Cuflon, εr = 2.17	5.9	PP on the substrate	Rectangular	3	
[72]	21.3 x 20 x 1.58	Dielectric, εr = 2.55	1	PP around the patch	Square	1	
[73]	60 x 55 x 8.3	FR4, εr = 4.4, tanδ = 0.02	5.4	PP around the patch	Circular	1	
[74]	75 x 75 x 1.6	FR4, εr = 4.4, tanδ = 0.0009	1.34	PP around the patch	Square	1	

recorded in [80] when two sets of symmetrical shorting pins are placed above the patch.

B. ADVANCED TECHNIQUES

In this section, many artificial materials that are proposed to improve the gain of low-band (up to 3 GHz) MPA are discussed by dividing them into two groups, namely electromagnetic-band gap and Metamaterials and Metasurfaces. These artificial materials are loaded on the ground plane, on the patch, used as a substrate, and superstrate to enhance the performance of the MPA [88][89][90][91]. Several metamaterials and metasurfaces such as split-ring resonator (SRR), modified SRR, complementary SRR (CSRR), open CSRR, composite right/left-handed (CRLH), artificial magnetic conductor (AMC), frequency selective surface (FSS), non-zero refractive index metasurface structure (NZRI MSS), metamaterial reflective surface (MRS), and partial reflective surface (PRS) are discussed to find better options for improving the gain of the TCAS directional antenna. In most of the advanced techniques, the gain and the radiation pattern shape of the antenna depend on the spacing between substrate-superstrate, and the superstrate thickness.

The proper selection of these parameters would therefore produce the significant gain increase when the combination of antenna and superstrate structure (multilayered) is perceived as a multi-sectioned transmission line (TL) along with the resonant lengths [92].

1) ELECTROMAGNETIC-BAND GAP (EBG)

Microstrip patch antennas placed on the substrate could emit very little amount of power towards the free space due to the power loss/leak through the substrate, and to improve the gain of an antenna, these power loss must be interdicted [93]. The use of EBG will direct the EM waves towards the main beam direction there by increasing the gain. EBG is an arrangement of dielectric elements as 1, 2, or 3D manners [94], [95]. It hinders the propagation of EM waves at specific incident angles at certain frequencies, and such frequencies are termed as partial band-gap [96]–[99].

At a certain frequency band, EBG will restrict the propagation of EM waves completely in all directions and that frequency band is known as global or complete band gap [100]–[102]. At this frequency band, all the EM waves will get reflected and the entire system will work as a mirror
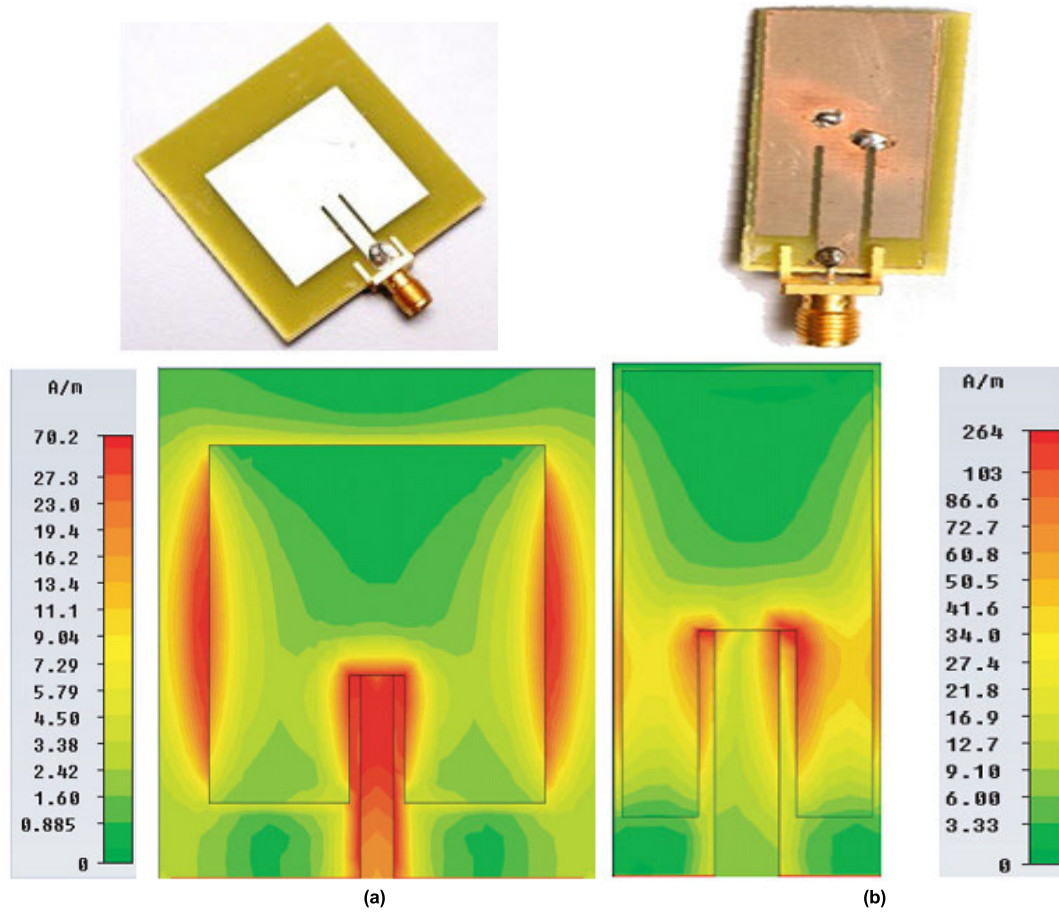
FIGURE 17. The MPA with and without shorting pins (a) conventional patch antenna and its current distribution (b) shorted microstrip patch antenna and its current distribution (2 shorting pins) [78].
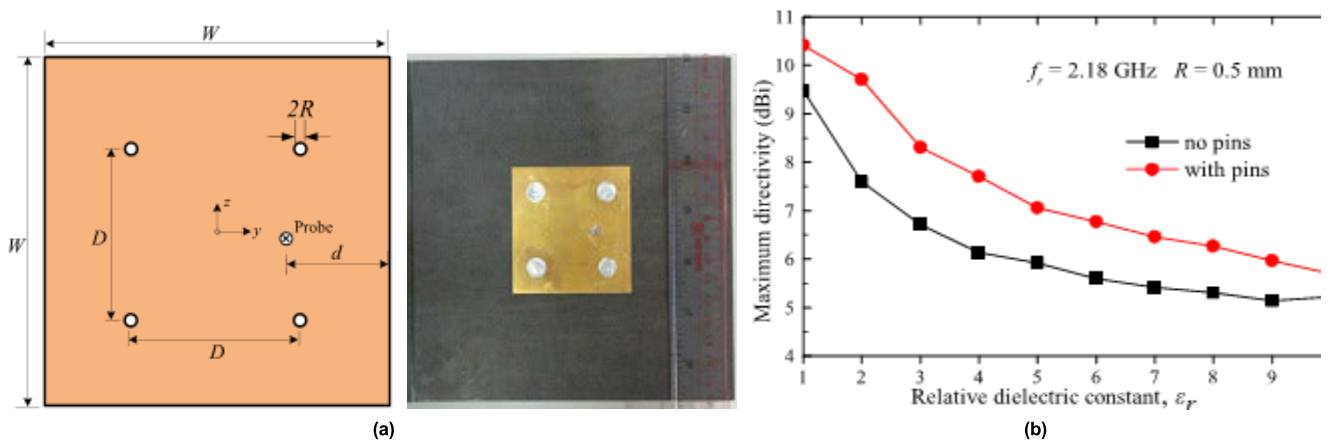
FIGURE 18. Fabricated prototype of the proposed antenna (a) top view of the square patch antenna with four shorting pins (b) gain plot of the patch antenna with and without pins [80].

[103], and it behaves as a transparent medium for other frequency bands as illustrated in Figure 20. As shown in Figure 21, the inclusion of 3 × 4 EBG elements (printed using inkjet technology) on a monopole microstrip antenna has increased the gain by 8.44 dBi in [104], and this structure

is designed mainly for wearable applications. The addition of the cylindrical EBG [105] and spiral EBG [106] structure to the rectangular patch antenna increased the gain by 0.5 dBi and 0.16 dBi, respectively. The disk-shaped EBG consists of six sectors integrated with the microstrip patch

FIGURE 19. Fabricated prototype of the rectangular patch antenna (a) geometry of the proposed antenna with a slot and a pair of shorting pins (b) photograph of the conventional and proposed patch antenna (c) gain vs. slot length plot of proposed antenna [81].

antenna [107], and the use of the switching vias on each sector improved the potential of EBG to control the radiation beam direction of the antenna, which in turn improved the gain by 8 dBi. In contrast to the conventional rectangular microstrip antenna, the etching of 3×3 cross-shaped EBG slots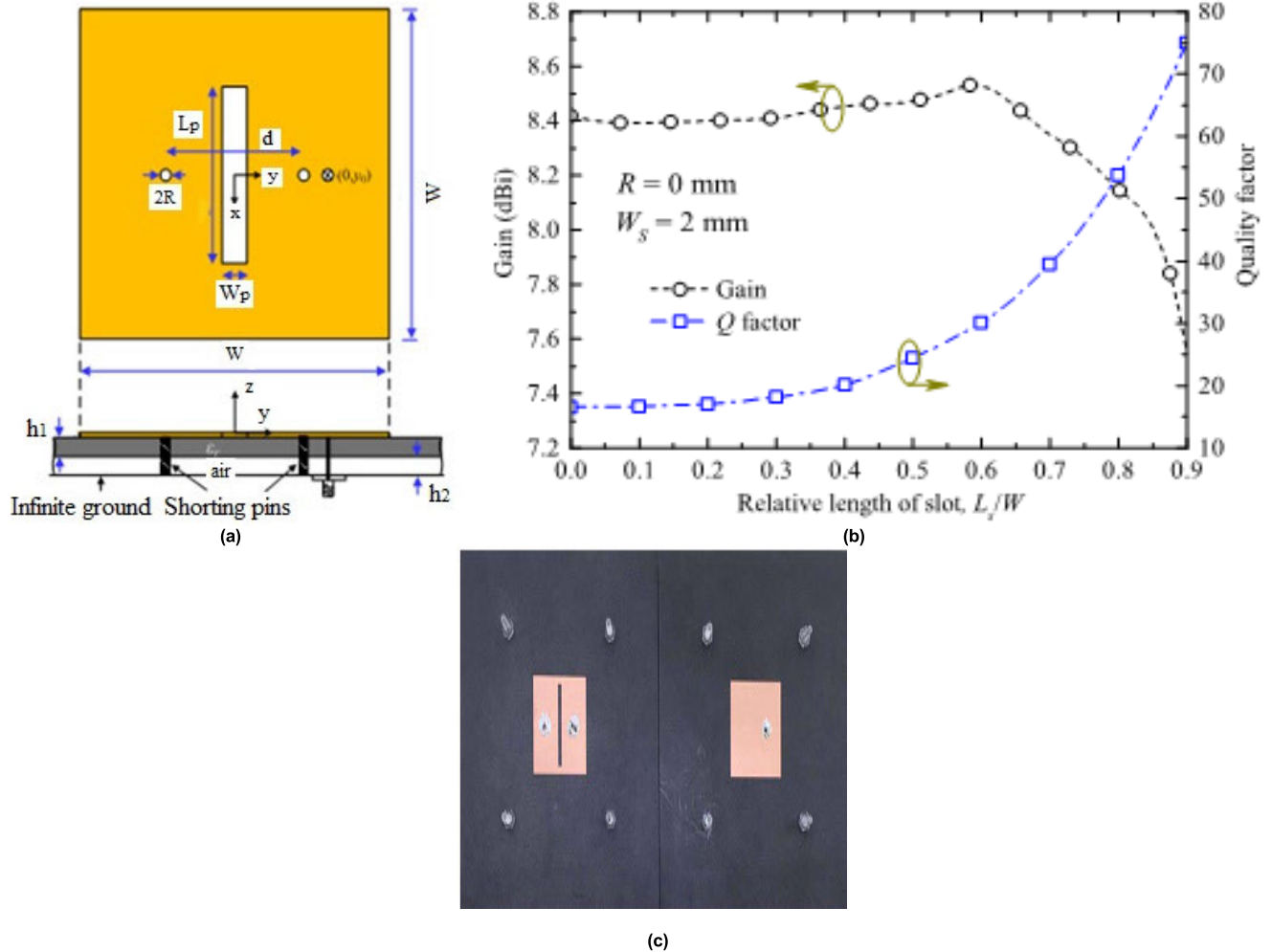 on the ground plane increased the gain by 8.2 dBi in [108]. The use of the shorting post on the slotted EBG ground plane significantly improved both the gain and efficiency of the stacked rectangular patch antenna for the road-vehicle communication application [109].

In [110], the cylindrical electromagnetic-band gap structure is etched on the circular microstrip patch antenna substrate, the proposed EBG structure consists of metallic rings and grounding vias to generate both radial and circular periodic structures as shown in Figure 22(a) & (b). As illustrated in Figure 22(c), for the matched frequency band which is between 2.56 to 2.65 GHz, the gain deviation of the patch antenna without and with EBG is 6.2 to 6.43 dB, and 8.1 to 9.33 dB. The maximum gain of the antenna without and with

the EBG is 6.43 dB and 9.33 dB at 2.65 GHz, therefore the gain of 2.9 dB has been improved by the addition of the EBG. In [111], the mushroom-shaped EBG is placed around the circularly polarized MPA as shown in Figure 23, the spiral-shape and arrangement of the EBG unit cells around the patch significantly improved the axial ratio and the gain of the patch antenna compared to the conventional antenna. The gain of the patch antenna has been improved by placing both mushroom and springboard EBG structure around the patch in [112]. In [113],the etching of 9×9 circular-shaped Photonic band gap (PBG) on the rectangular patch antenna substrate has increased the gain up to 10 dBi. The MPA with cylindrical EBG structure has been developed and validated for gain enhancement in [114].

A number of gain enhancement ideas for patch antenna were addressed in [115] and the use of PBG defect resonator and high dielectric constant superstrate methods increased the gain by 20.3 dBi and 16 dBi, respectively, therefore these two are considered to be the most important techniques.

TABLE 4. Summary of research on gain enhancement of MPA using shorting pins.

| Ref	Dimension (mm³)	Dielectric substrate	Gain enhancement (dB)	Shape of shorting pins	No. of pins	Gain enhancement technique	Freq. band
[80]	60 x 60 x 3.175	Rogers RT/ Duroid 5880, εr = 2.2, tanδ = 0.0009	2.8	Circle	4	Two sets of SP are placed symmetrically above the patch	
[81]	115 x 115 x 1.57	Rogers RT/ Duroid 5880, εr = 2.2, tanδ = 0.0009	1.7	Circle	2	Placed on the patch between two longitudinal sides of a slot	
[82]	170 x 170 x 3.175	Rogers RT/ Duroid 5880, εr = 2.2, tanδ = 0.0009	2.9	Circle	4	Placed symmetrically beneath the patch	LOW FREQ BAND
[83]	Rg = 175, Rp = 48, h = 2.5 mm	F4B, εr = 3.0, tanδ = 0.002	2	Circle	16	Placed on the patch	(Up to 3GHz)
[84]	100 x 100 x 3.175	Arlon, εr = 2.5, tanδ = 0.003	2	Circle	4	Placed on the patch	
[85]	150 x 150 x 3.175	Rogers RT/ Duroid 5880, εr = 2.2, tanδ = 0.0009	2.8	Circle	8	Two sets of SP are placed symmetrically above the patch	
[86]	Rg = 90, Rp = 33.25, h = 3.17 mm	Rogers RT/ Duroid 5880, εr = 2.33, tanδ = 0.0009	1.98	Circle	19	Placed on the patch	
[87]	60 x 60 x 1.6	FR4, εr = 4.4,tanδ = 0.02	1.2	Circle	1	Below the patch	
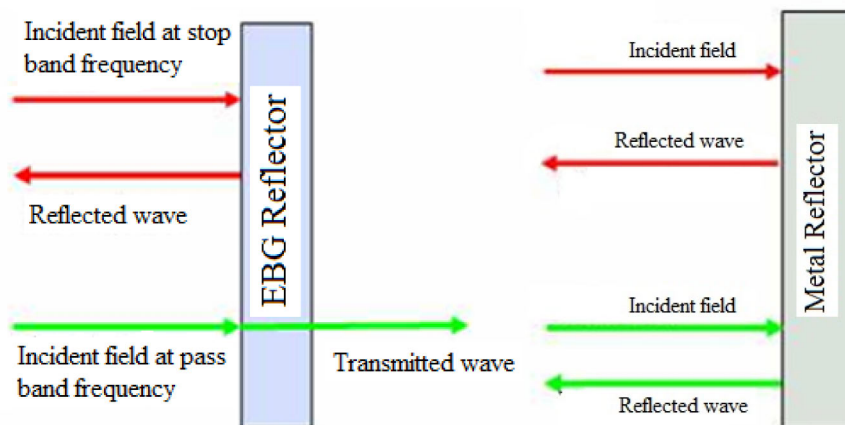
FIGURE 20. The comparison of EBG and the metal reflector [103].

In [110],[111], [116]–[119], mushroom-shaped EBG structures have been proposed to improve the gain and efficiency of the printed antennas, and in [120], [121] unipolar compact-photonic band gap (UC-PBG) unit cells are used to improve the gain of aperture-coupled fed printed antennas. Eventually, many authors have also used EBG as a superstrate to improve the gain of MPA [115], [122]–[124].

The previous research work [104], [115] on the gain enhancement of MPA using EBG is summarized in TABLE 5. The work that has been reviewed under the EBG technique is for the low-frequency band and the dimension of all selected work is within the assigned size of the TCAS antenna. To increase the gain of the patch antenna, different shapes of the EBG elements are loaded onto the ground plane, around

the patch, and used as a superstrate. The maximum gain increase of 8.44 dBi [104] is reported when 4 × 3 EBG elements are loaded onto the ground plane of the patch antenna.

2) METAMATERIALS AND METASURFACE
Metamaterials can be considered as artificially fabricated materials having some salient electromagnetic properties such as negative refractive index, negative permittivity, and negative refractive index, n [125], [126]. Metamaterials have been employed primarily for applications such as performance enhancement of couplers and MPA [127]–[129]. Metasurface has recently been of great interest to researchers and has been employed in a variety of fields, including antennas and optics [130], [131].
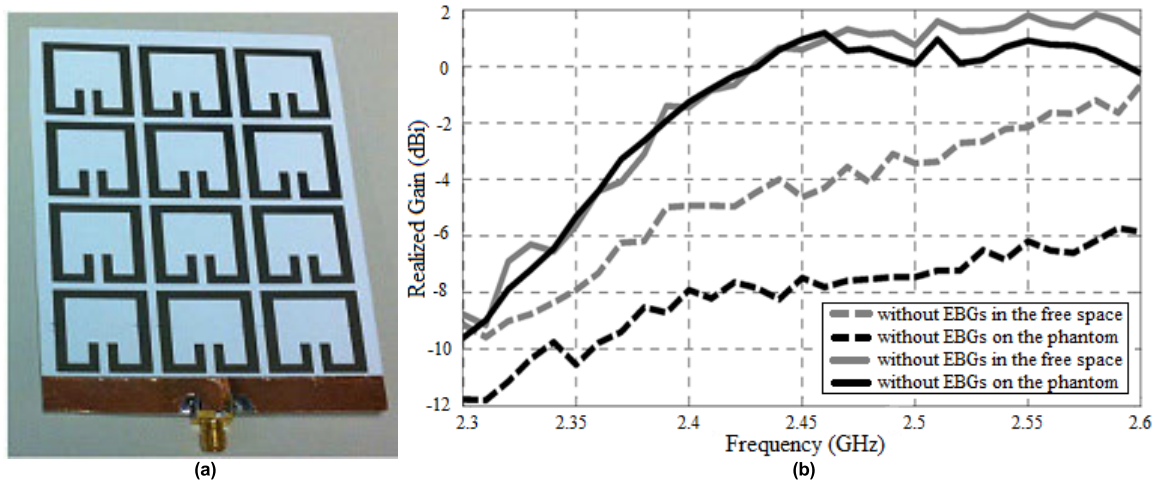
FIGURE 21. Fabricated prototype of microstrip monopole antenna (a) loaded with 3 × 4 EBG array (b) gain plot of with and without EBG unit cells for air and phantom [104].
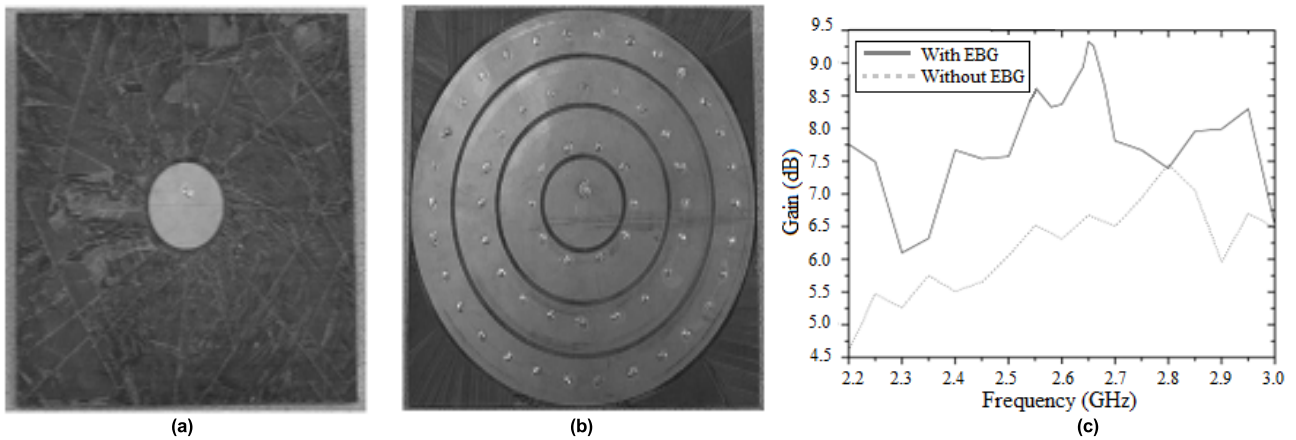

FIGURE 22. Proposed circular patch antenna with EBG substrate (a) with classical substrate (b) with a cylindrical EBG substrate (c) Gain plot of circular patch antenna with classical and cylindrical EBG substrate [110].

One of the salient features of metamaterials is that they enable the control of direction and power emission over small solid angle for patch antennas. The principle behind this is that the effective permittivity or permeability will become zero as the resonant frequency equals the plasma frequency and this causes the refractive index n to become zero [132].

$$\text{Refractive Index}, n = \sqrt{\varepsilon_{eff}\,\mu_{eff}} = 0 \qquad (4)$$

As per Snell's law, when a source is placed on the substrate with zero refractive indexes, the refracted ray flows very near to the surface normal. Therefore, the entire refracted rays will be in the same direction around the normal. Hence, better directivity can be achieved when the operating frequency equals the plasma frequency [133], [134].

In the last decade, the scientific community has shown great interest in the study of metamaterials. An array of left-handed metamaterial (LHM) is integrated with the patch in [135], [136], to study the effect of metamaterial on patch antenna at lower frequency band. The E-field distribution

of a patch antenna with and without LHM is illustrated in Figure 24.

The use of LHM has made the radiation distribution more directive which shows its ability to focus the radiation beam in a particular direction. Here, the inclusion of 7 × 8 LHM on the patch has improved the gain by 4 dB which is illustrated in Figure 25. Two planar antennas in which antenna 1 is integrated with five symmetrical CRLH cells and antenna 2 is integrated with 10 asymmetrical CRLH cells were proposed in [137]. As seen in Figure 26, the d-shape slots are etched from both the patches, and the spiral-shaped tail ends are grounded using holes. Figure 26(c) illustrates the gain and efficiency of both antennas. The maximum gain and efficiency of antenna 1 at 2GHz are 1.5dBi and 35%, for antenna 2, the gain and efficiency are 3.5dBi and 60%, which means that the use of 10 asymmetrical CRLH cells has increased the gain and efficiency by 2dBi and 25%.

Various metamaterials such as MSRR [139], [140], OCSRR [141], S-shape metamaterial [142], CRLH [137],
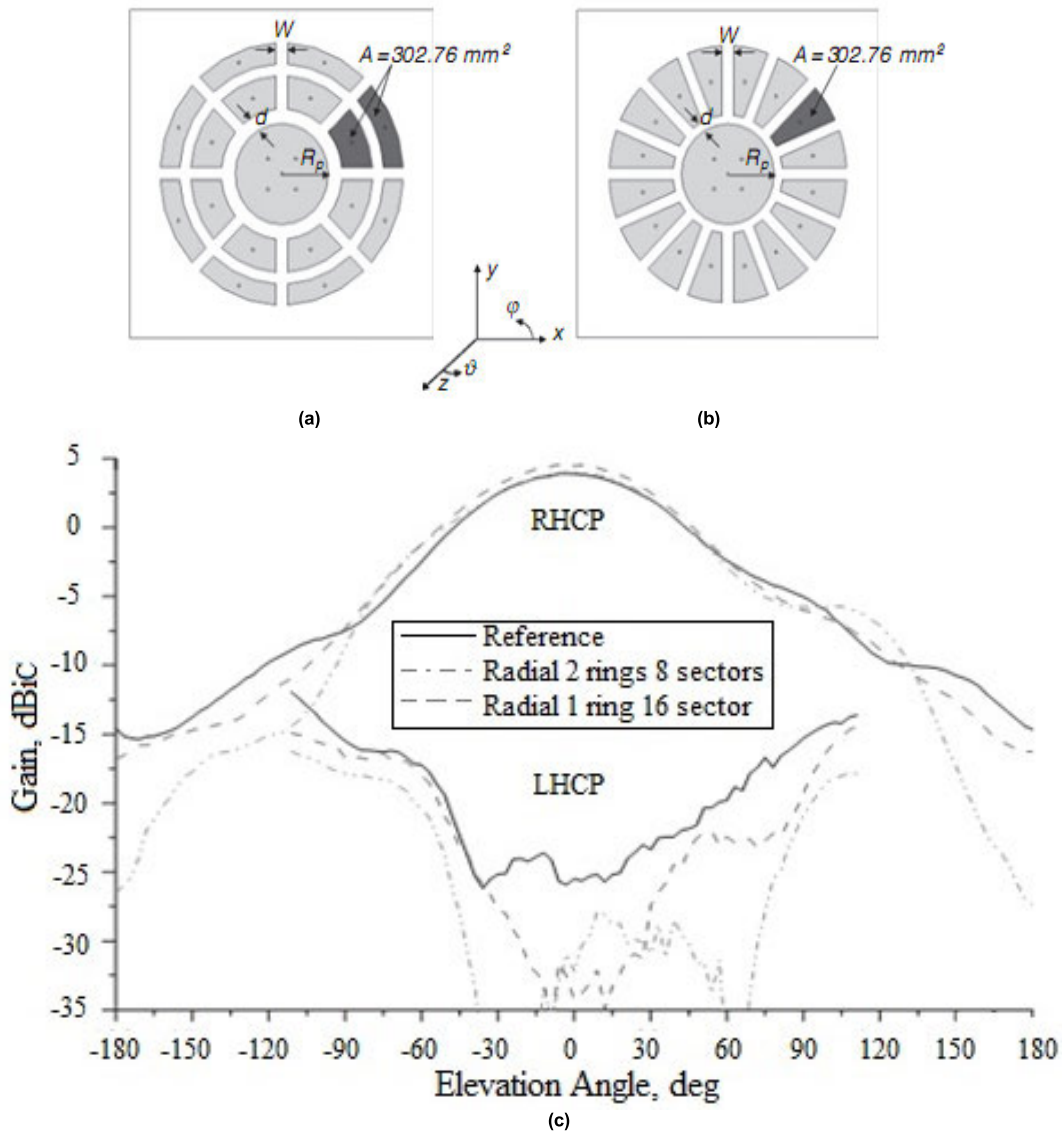
FIGURE 23. Proposed circular patch antenna with EBG unit cells (a) two-rows of EBG unit cells around the circular patch antenna (b) single-row EBG unit cell around the circular patch antenna (c) comparison of RHCP and LHCP radiation pattern at 1.575GHz [111].

AMC [143], and MRS [144] are loaded on the patch, and in [145], [146] [147], [148] metamaterials such as CSRR, AMC, and PRS are loaded on the ground plane to improve the gain of the MPA. The metamaterials such as SRR [138] [149] [150], closed ring [151], [152], MSRR [153], AMC [154]–[157], and FSS [158] are used as superstrate, AMC [159] is loaded on the substrate, and materials like NZRI MSS [160], FSS [161] are loaded below the patch. A nested split-ring resonator (SRR) is used to improve the gain of MPA, this metamaterial structure generates a negative refractive index over the frequency band of 770MHz to 1070MHz This refractive index layer will be used as a superstrate over the C-shaped MPA as shown in Figure 27, and it is noted that this approach has improved the gain by

2.64 dBi. In [154], two different metasurfaces that are single-layer artificial magnetic conductors (AMC) and double-layer reactive impedance surfaces (RIS) are used to improve the gain of the MPA. Figure 28 shows the radiation pattern of circularly polarized components (LHCP and RHCP) in the azimuthal plane that is $\Phi = 0^0$ and $\Phi = 90^0$, and it has been noted that the radiation pattern of the antenna is stable with the frequency band and has improved the gain by 0.9 (AMC) and 1.1 dB (RIS). A novel Non-zero refractive index metasurface structure (NZRI MSS) is used to improve the gain of MPA in [160] and is placed at the bottom side of the patch antenna as shown in Figure 29. This method has improved the gain by 2.04 dBi (6.21 to 8.25 dBi), 2.53 dBi (6.52 to 9.05 dBi), and 1.61 dBi (10.54 to
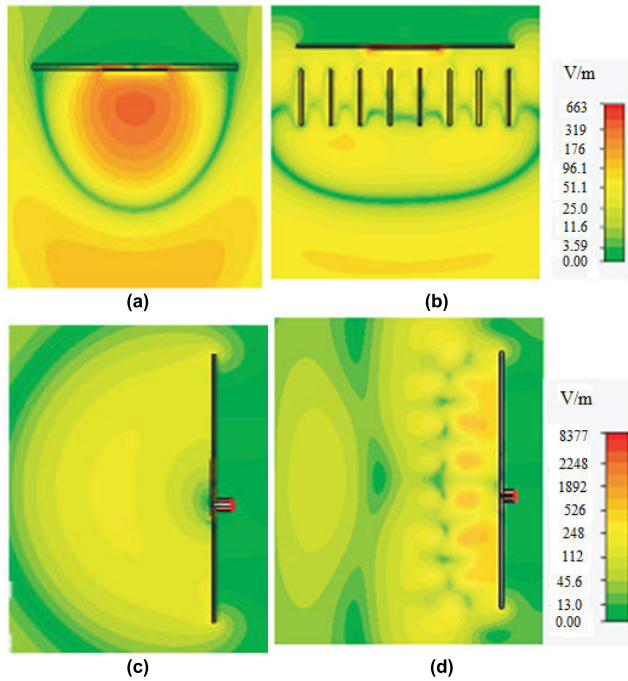
FIGURE 24. E-field distribution in E and H plane (a) & (c) For MPA (b) & (d) For MPA integrated with LHM [135].

FIGURE 25. Fabricated prototype of MPA (a) with LHM (b) gain plot of patch antenna with and without LHM [135].

12.15 dBi) at 0.6 GHz, 2.5 GHz, and 4.8 GHz. In addition to gain and directivity improvement, it has also resulted in a good directional radiation pattern than the conventional patch antenna.

The 6×6 Frequency Selective Surface (FSS) elements are loaded under the patch as shown in Figure 30, this approach has increased the gain between 3 and 4 dB compared to the traditional MPA without FSS [161]. A number of research work [135]–[161] on the gain enhancement of MPA using metamaterials (MTMs) and metasurface has been summarized in TABLE 6. The work that has been reviewed under the MTMs and metasurface method is for the low-frequency band and the dimension of all selected work is within the assigned size of the TCAS antenna. To improve the gain of the MPA, different shapes of the MTMs and metasurface elements are loaded onto the ground plane, around the patch, used as a substrate, and superstrate. The gain increase of 5.68 dBi [136] is reported when 5×7 SRR elements are loaded on the patch.

V. DISCUSSION
The characteristics and limitations of many traditional and advanced gain enhancement techniques reviewed above to enhance the gain of TCAS directional antennas will be discussed here. Since the allotted frequency band for TCAS application is L-band (1.09GHz for Transmission and 1.03GHz for Reception), we reviewed a wide range of papers (frequency range is up to 3GHz) with different enhancement techniques such as parasitic patches, shorting pins, energy-band gap, metamaterials, and metasurfaces.

The parasitic patches (PPs) is an effective approach to increase the gain of MPA. It is important to have a clear understanding of the placement of PPs to improve the gain of the MPA. When the parasitic patch (PP) is positioned above or below the driven patch and the separation gap is approximately half a wavelength ($\lambda/2$), the standing wave that contributes to the main radiation is excited inside the leaky resonant cavity that is created between the two patches and greatly improves the gain when it interacts with the driven patch cavity. The air gap thickness which separates the driven and the PPs would have a significant impact on the antenna gain. In [61], comprehensive work has been done to find the ideal air gap thickness for the antenna operating at 1.6 GHz to achieve substantial gain improvement, it has been noted that, when the air gap thickness is 30 mm, an increase of 3.3 dB has been recorded and an increase of 2.2 dB has been recorded when the air gap thickness is 20 mm. In many research works, the thickness of the PP substrate layer is increased in order to improve the antenna gain. In [60][62], the addition of a single and double PP above the feed patch increased the gain by 1.8 dB, and 2.5 dB in contrast to a single patch antenna when the separation gap between the main and the parasitic patch is

FIGURE 26. Fabricated prototype proposed antenna (a) antenna 1 with of 5 symmetrical MTM cells and d-shaped slots (b) antenna 2 with 10 asymmetrical MTM cells & d-shaped slots (c) gain plot of the proposed antenna [124].

$\lambda 0/2$, the parasitic patch substrate thickness is around 0.5 λ_g (where λ_g is dielectric wavelength), an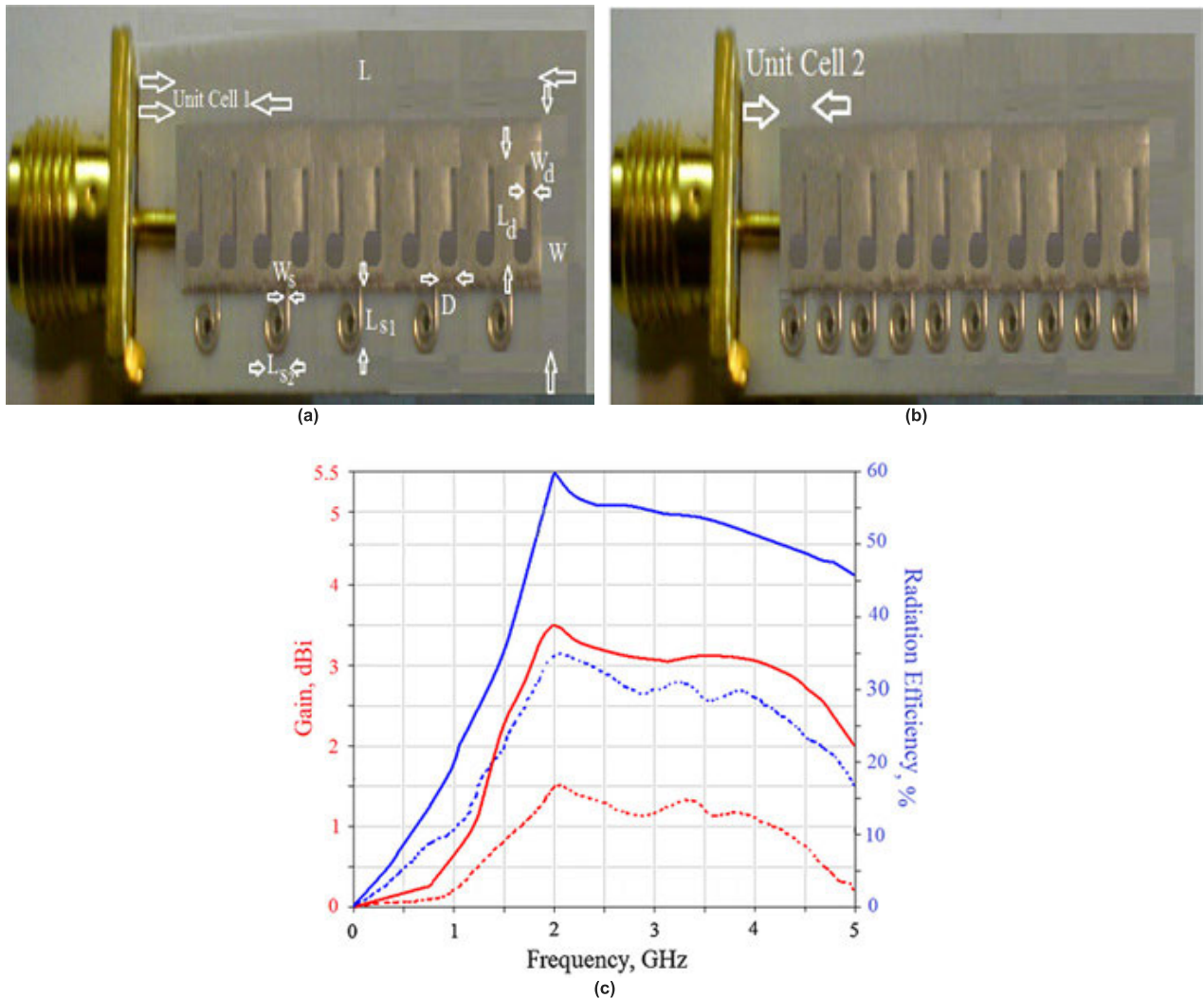d the ratio of the length of the parasitic patch (L_p) to the length of the feed patch (L_f) is 1.0. In [59], a maximum gain of 2.61 dB is achieved when the two PPs are placed between the driven patch, the separation gap between the top PP layer and the fed patch is 0.36 dBi, and the separation gap between the bottom PP layer and the fed patch is 0.15 dBi. After reviewing a lot of research work on improving the gain of MPA using a parasitic patch, we could finally see the different parameters that need to be taken care of (with reference to previous work, to improve the gain, the separation gap has to be $\lambda 0/2$, the parasitic patch substrate thickness has to be 0.5 λ_g, and the length of the parasitic patch and the driven patch must be the same).

Although the parasitic patch technique is simple and an effective enhancement method, there are some drawbacks, such as geometric complexity, difficulty in designing due to radiative/non-radiative patch elements, a thick parasitic patch substrate, a large ground plane which increases back and side-lobe levels, and the need for a large area due to stack structure.

The shorting pins will electrically short the patch layer to the ground plane. The working of shorting pins are analogous to the parallel inductors hence it extremely perturbs the distribution of the field below the patch. Four metallic shorting pins are placed on two diagonals of a square MPA [71]. The addition of shorting pins will shift the resonant frequency and the free-space wavelength. It is noted that the gain enhancement using shorting pins will generally get affected by the relative permittivity of the substrate (ε_r), the aspect ratio of the patch (W/L), and frequency tuning ratio (f_r/f_o). In a lot of research work, it is reported that the gain and the resonant frequency is a function of pin-to-pin spacing (D/W). The gain and the resonant frequency remain the same as the conventional patch when all the selected shorting pins are placed at the center point of the patch (i.e. /W=0). As the spacing increases from 0 to 1, initially, both resonant frequency and gain will increase
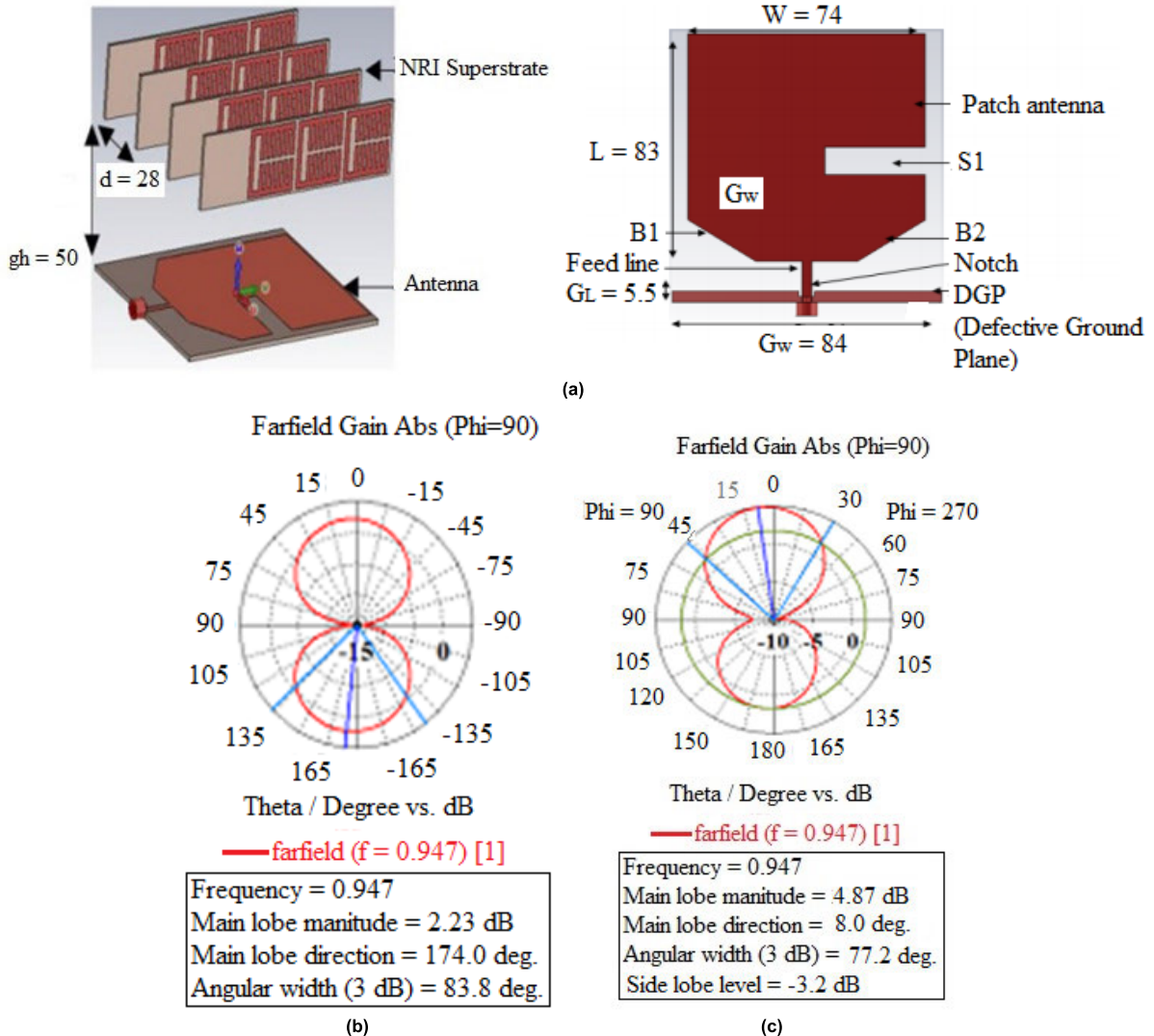
FIGURE 27. Fabricated prototype of the MPA (a) MPA with NRI superstrate (b) gain radiation pattern of typical patch antenna (c) gain radiation pattern of C-shaped patch antenna with NRI superstrate [138].

and attains their maximum value when D/W = 0.71, but after this threshold value both parameters will gradually decrease. At D/W = 0.71, the maximum gain of 9.4 dB has been recorded which is a 1.9 dB improvement compared to the conventional patch design without shorting pins. To analyze the effect of ε_r over the gain, the value of ε_r is varied from 1 to 4 by keeping the spacing value constant at 0.71, the increase in ε_r has gradually decreased the gain from 9.4 dB to 7.7 dB. In [75], in addition to four shorting pins which are kept at a spacing distance of 0.71 from the center, another four shorting pins were placed at a distance of 0.5 from the center, and these additional shorting pins have further improved the gain by 0.7 dB.

In this approach, input impedance depends mainly on the spacing distance between the pin and the probe. Although a lot of research work has been done to find the optimum location of the pin for 50Ω feed line, no comprehensive anal-

ysis has been carried out to provide insight into how shorting pins can decrease the input impedance. The asymmetrical properties of the shorting pins degrade the cross-polarization of the MPA in the H-plane. In short, this approach improves the gain of the MPA at the expense of a wide patch area.

The principle of electromagnetic-band gap (EBG) is derived from the photonic-band gap (PBG) method used in optics due to its similar properties with respect to wave propagation and wave suppression at different frequency ranges known as band gap [69], [162], [163]. This approach is a breakthrough in improving the performance of the MPA, and these structures will improve the antenna gain by suppressing the surface wave effect. The EBG structures are very sensitive to the substrate thickness, the permittivity of the substrate, and the geometry of the EBG. The key characteristics of the EBG structures are the suppression of the surface wave within the given band gap range, and its ability to direct and monitor

TABLE 5. Summary of research on gain enhancement of MSA by electromagnetic-band GAP (EBG).

Ref	Dimension (mm^3)	Dielectric substrate	Gain enhancement (dB)	Gain enhancement technique	Shape of EBG element	No. of EBG element	Gain increase @ no. of band	Freq. band
[104]	127 x 87 x 1.3	Dielectric, εr = 3.2, tanδ =0.07	8.44	Loaded on the ground plane	Open square ring	4 x 3	1	
[105]	100 x 100 x 3.2	Rogers RT/ Duroid 5880, εr = 2.2, tanδ = 0.0009	4.86	Holes in dielectric	Cylindrical	16	1	
[106]	53 × 53 × 1.524	ArIon A 450, εr = 4.5	0.6	Loaded on the ground plane	Rectangular spiral	5 x 5	1	
[107]	D=115.4, t=3.2	FR4, εr = 4.4,tanδ = 0.02	8	Loaded on the ground plane	Circular	6 x 7	2	
[108]	27 ×36 x 1.6	Dielectric, εr = 4.28	8.2	Loaded on the ground plane	Cross-shape	3 x 3	1	
[109]	40 x 40 x 1	FR4, εr = 4.4, tanδ = 0.018	1.17	Loaded on the ground plane	Square	8 x 8	1	*LOW FREQ BAND* *(Up to 3GHz)*
[110]	180 x 180 x 3.2	Taconic, εr = 2.55	2.9	Loaded on the ground plane	Cylindrical shape	60	1	
[111]	110 x 110 x 1.58	Taconic CER10, εr = 10.0, tanδ = 0.035	0.6	Around the patch	Radial	2 x 8	1	
[112]	40.7 x 40.7 x 3	FR4, εr = 4.4,tanδ = 0.02	2.63	Around the patch	Square (Springboard)	64	1	
[113]	52 x 25.96 x 1	Dielectric, εr = 10	10	Used as a superstrate	Circular	9 x 9	1	
[114]	38 x 30.9 x 1.57	FR4, εr = 4.4, tanδ = 0.018	1.68	Used as a superstrate	Cuboids & slotted cylinders	3 x 3	2	
[115]	70 x 70 x 3.18	Rogers RT/ Duroid 5880, εr = 2.2, tanδ = 0.0009	11.3	EBG and metamaterial as superstrate	Slotted square	7 x 7	1	

the propagation of EM waves, which enhances the MPA performance by reducing back radiation, and cross-polarization. In [164], [165], the MPA was surrounded by a square grid of tiny metal pads along with the ground vias, popularly known as the mushroom structure, a significant reduction of surface waves was observed in the substrate, which greatly enhanced the MPA gain. In [115], a thick substrate was replaced by an EBG substrate, and a maximum gain improvement of 7.2 dB was reported. The major drawbacks of this approach are the need for exceptionally high periodicity, a substantial increase in height, geometric complexity, and a complication in a straightforward design.

Various types of artificial materials have been proposed to improve the gain and directivity of the patch antenna [147], [162], [163], [166]–[169]. Artificial magnetic conductor (AMC) with partial reflective surfaces (PRS) has recently been proposed to overcome the challenges of the EBG approach, such as high dimension and low gain. Even though it minimizes overall thickness and improves gain, it still suffers from low aperture efficiency. A very simple and effective gain enhancement technique is the use of a thick substrate which improves total power efficiency in the direction of the surface wave. However, the substantial increase in direct radiation power would degrade the effi-

ciency and the radiation pattern of the antenna. A comprehensive study on split-ring resonator (SRR) to enhance gain and directivity where the Snell-Decartes laws are used with a non-zero refractive index (NZRI) was discussed in [170]. The most attractive characteristics of NZRI metamaterials are the propagation of EM waves with non-zero phase values within the zero refractive index (ZRI) medium. The essential features of the NZRI metasurface structure (MSS) are ease of fabrication, low-profile, and low mutual coupling.

Most of the previous research work has used traditional techniques such as parasitic patches and shortening pins to increase TCAS directional antenna gain, and very few or no work has been recorded to date using advanced methods such as EBG, FSS, metamaterials, and metasurface. In this review article, we discussed most of the advanced methods used so far to increase the gain of the MPA for a frequency range of up to 3GHz. The advantages and disadvantages of traditional and advanced gain enhancement techniques are discussed in this section and it is noted that the gain of the MPA depends on so many factors. As all the research work reviewed in this study is limited in terms of operating frequency and size, these techniques are very well suited to improve the gain of the TCAS directional antenna.

TABLE 6. Summary of research on gain enhancement of MPA using MTM and metasurface.

Ref	Dimension(mm³)	Dielectric substrate	Gain enhancement (dB)	Gain enhancement technique	MTM used for gain enhancement	No. of MTM unit cells	Gain increase @ no. of band	Freq. band
[135]	117 x 127 x 41.6	FR4, εr = 4.7,tanδ = 0.019	4	Patch loading	SRR	8 x 7	1	
[136]	59 x 42.4 x 1.6	FR4, εr = 4.7,tanδ = 0.019	5.68	Patch loading	SRR	5 x 7	1	
[137]	25 x 10 x 1.6	Rogers RO4003, εr = 3.38,tanδ = 0.0022	2	Patch loading	CRLH	5 & 10	1	
[138]	83 x 74 x 1.6	FR4, εr = 4.7,tanδ = 0.019	2.65	Superstrate	SRR	4 x 3	1	
[139]	45.25 x 36 x 1.6	FR4, εr = 4.4,tanδ = 0.02	3.69	Patch loading	Modified SRR	3 x 3	2	
[140]	24.72 × 22.8 × 1.6	FR4, εr = 4.4,tanδ = 0.02	3.63 & 1	Patch loading	Modified SRR	5 x 4	2	
[141]	40 x 30 x 1.5	FR4, εr = 4.4,tanδ = 0.02	1.4, 1.7	Patch loading	Open complementary SRR	1	2	
[142]	45 x 50 x 0.787	RT/duroid 5880, εr = 3.38,tanδ = 0.0022	1.8	Patch loading	S-shape	3 x 6	1	
[143]	60 × 60 × 1.6	FR4, εr = 4.4,tanδ = 0.02	2.138	Patch loading	AMC	3 x 2	2	
[144]	33.2 x 37.8 x 1.6	FR4, εr = 4.7,tanδ = 0.019	1.1	Patch loading	MRS (MTM reflective surface)	4 x 4	2	
[145]	40 x 46 x 1.6	FR4, εr = 4.4,tanδ = 0.02	1.13	Ground plane loading/etching	CSRR	2 x 2	1	
[146]	60 × 60 × 1.6	FR4, εr = 4.4,tanδ = 0.02	4.95, 3.88, 4.13	Ground plane loading/etching	AMC	4 x 4	3	LOW FREQ BAND
[147]	64 × 64 × 1.6	FR4, εr = 4.4,tanδ = 0.02	2.39, 3.07, 3.58	Ground plane loading/etching	AMC	4 x 4	3	(Up to 3GHz)
[148]	69 x 69 x 1.6	FR4, εr = 4.4,tanδ = 0.02	2.6	Ground plane loading/etching	PRS	5 x 5	1	
[149]	74.5 x 40 x 1.6	FR4, εr = 4.7,tanδ = 0.019	1.907	Superstrate	SRR	3 x 4	1	
[150]	85 x 85 x 0.762	Rogers RO4350, εr = 3.48,tanδ = 0.004	3.4	Superstrate	SRR	10 x 10	1	
[151]	41 x 33.6 x 1	Dielectric, εr = 2.65,tanδ =0.001	10	Superstrate	Closed ring	9 x 9	1	
[152]	61.25 x 61.25 x 1.6	FR4, εr = 4.4,tanδ = 0.02	2.71	Superstrate	Closed ring	5 x 5	1	
[153]	36 x 36 x 0.762	Rogers RO4350, εr = 3.48, tanδ = 0.004	3.4	Superstrate	MSRR	10 x 10	1	
[154]	100 x 100 x 3.18	RT 6010/duroid, εr = 10.2, tanδ = 0.0023	1.2	Superstrate	AMC	4 x 4 8 x 8 10 x 10	3	
[155]	90 x 90 x 1.6	Rogers RT/ Duroid 5880, εr = 2.2, tanδ = 0.0009	1.73	Superstrate	AMC	6 x 6	1	
[156]	125 x 100 x 6.5	Rogers RO4003, εr = 3.38, tanδ = 0.0021	3	Superstrate	AMC	5 x 5, 5 x 4, 5 x 3	1	
[157]	70 x 50 x 3	FR4, εr = 4.4,tanδ = 0.02	4	Superstrate	AMC	6 x 9	2	
[158]	120 x 120 x 0.8	FR4, εr = 4.4,tanδ = 0.02	2.28 dBi	Superstrate	FSS	5 x 5	1	
[159]	100 x 120 x 1.6S	FR4, εr = 4.7,tanδ = 0.019	4	Substrate	AMC	5 x 6	1	
[160]	70 x 85 x 2	Ceramic-filled bioplastic, εr = 15	2.04 2.53 1.61	Below the patch	NZRI MSS	7 x 3	3	
[161]	150 x 150 x 1.6	FR4, εr = 4.4,tanδ = 0.02	3-4 dBi	Below the patch	FSS	6 x 6	1	
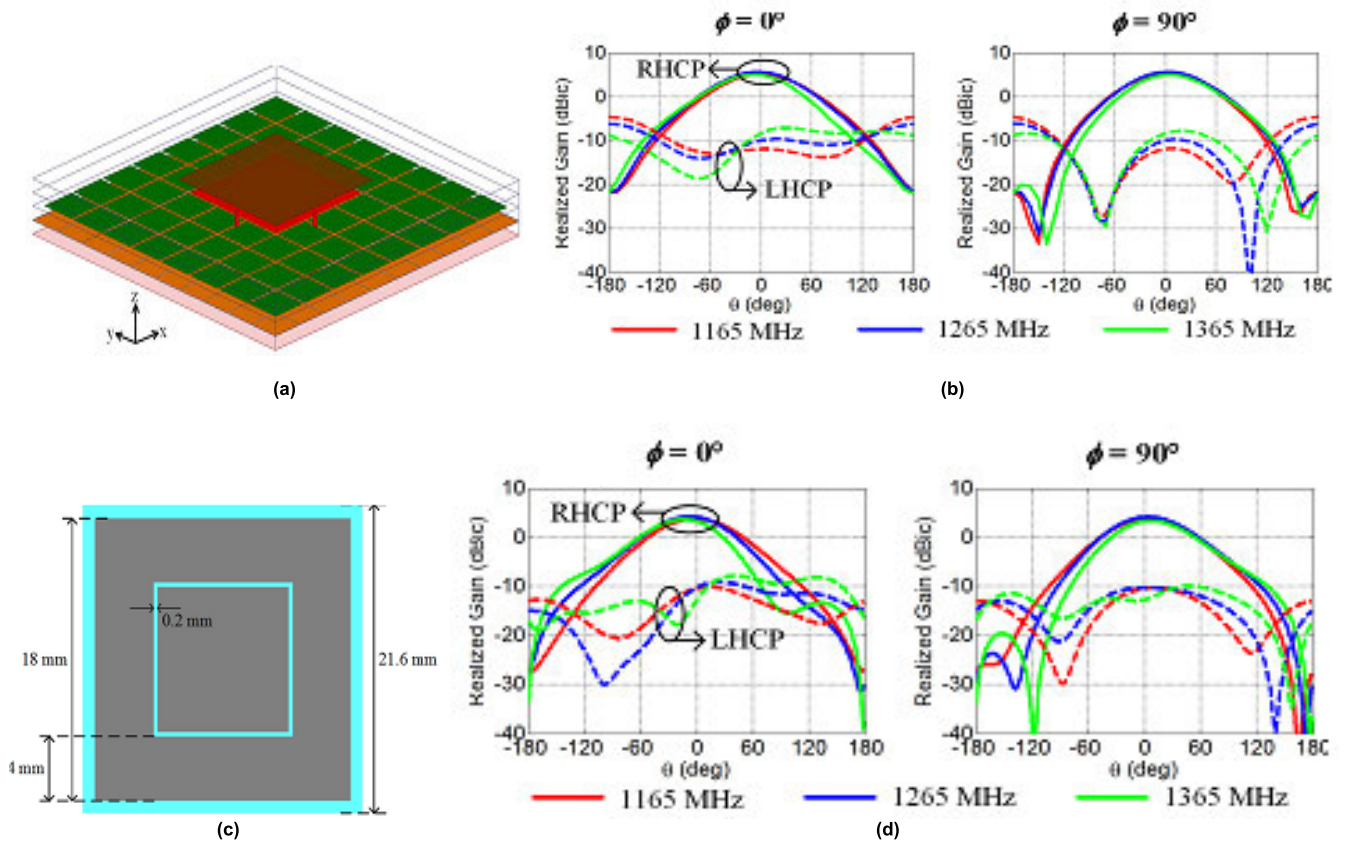
FIGURE 28. Fabricated prototype of proposed MPA (a) MPA with double-layer metasurface (b) the corresponding gain plot (c) MPA with double-layer AMC (d) the corresponding gain plot [154].
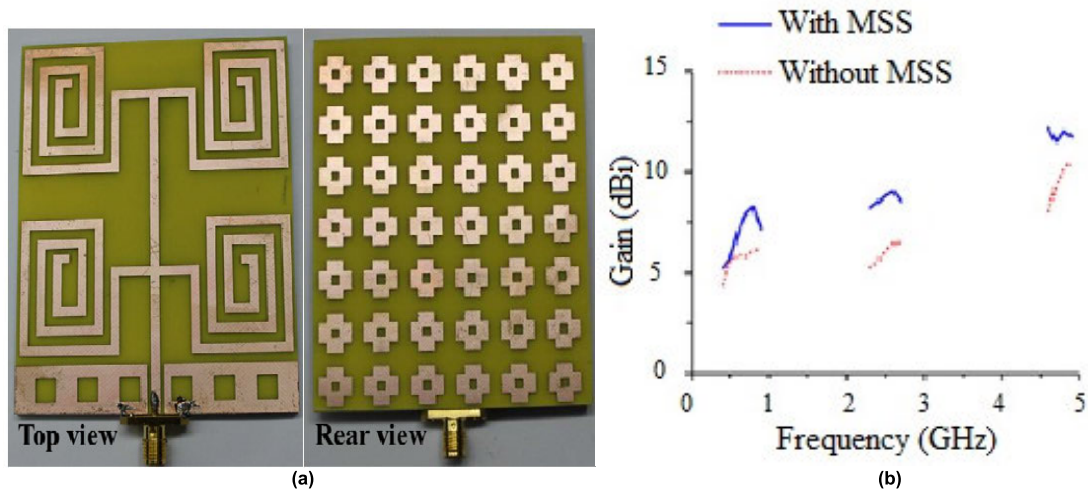
FIGURE 29. Fabricated prototype of the MPA (a) NZRI MSS-backed MPA (b) gain plot [160].

VI. CONCLUSION

In this review article, the concept of conventional TCAS directional antenna, which is an array of monopole antennas, was briefly discussed, highlighting its limitations such as low gain, high side-lobe level, and wider beam width. The

main focus of this paper is on gain enhancement techniques for TCAS directional antenna. Initially, several proposed methods for improving TCAS antenna gain were briefly analyzed and their limitations were discussed. It is noted that the majority of the work in the literature has replaced
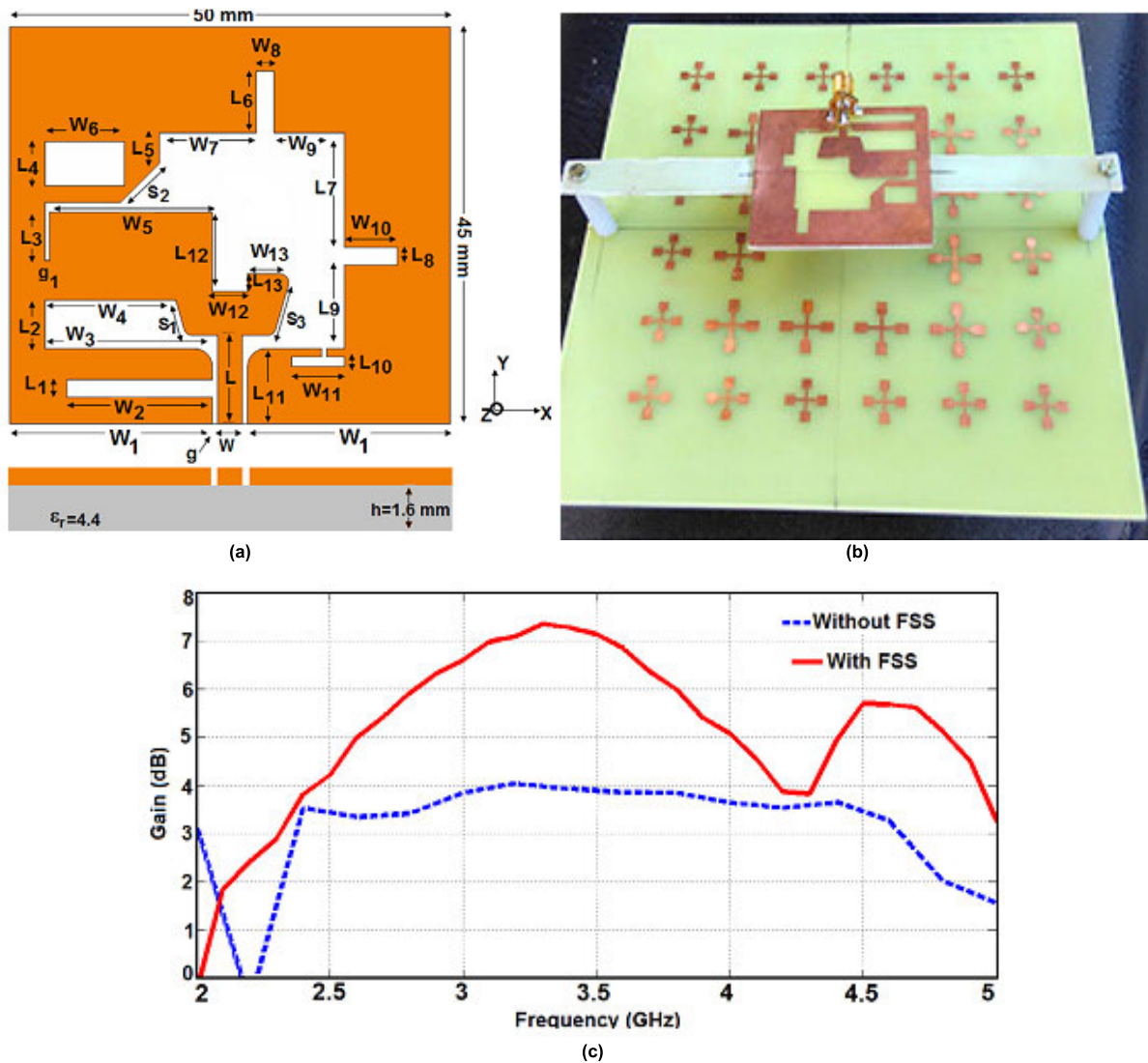
FIGURE 30. Proposed MPA structure (a) geometry of the MPA (b) fabricated prototype of proposed antenna with FSS (c) gain plot of the antenna with and without FSS [161].

the monopole antenna with MPA as it is highly suitable for airborne applications. In order to further improve the gain of the patch antenna, various gain enhancement techniques have been integrated with the antenna. Most of the reviewed work has used conventional methods, such as parasitic patches and shorting pins to improve the antenna gain, and therefore we have further assessed many advanced techniques proposed so far to increase the gain of the patch antenna that operates in the L and S bands and is, therefore, more appropriate for the TCAS application in particular.

REFERENCES

[1] J. E. Kuchar and A. C. Drumm, "The traffic alert and collision avoidance system," *Lincoln Lab. J.*, vol. 16, pp. 277–296, Nov. 2007.

[2] W. H. Harman, "TCAS: A system for preventing midair collisions," *Lincoln Lab. J.*, vol. 2, no. 3, pp. 437–458, 1989.

[3] M. J. Kochenderfer, J. E. Holland, and J. P. Chryssanthacopoulos, "Next-generation airborne collision avoidance system," *Lincoln Lab. J.*, vol. 19, no. 1, pp. 17–33, 2012.

[4] F. Romli, J. King, L. Li, and J.-P. Clarke, "Impact of automatic dependent surveillance-broadcast (ADS-B)on traffic alert and collision avoidance system (TCAS) performance," in *Proc. AIAA Guid., Navigat. Control Conf. Exhib.*, Aug. 2008, pp. 1–11.

[5] *TCAS S72-1735-25*, AIRNC 735, Sensor Syst. Inc., Aircr. Antennas Since 1961.

[6] M. R. Abraham, S. O. Kundukulam, and C. K. Aanandan, "An airborne VHF printed monopole antenna for platform constrained applications," *Prog. Electromagn. Res. M*, vol. 78, pp. 103–113, Jan. 2019.

[7] H. Zhai, D. Yang, L. Xi, and D. Feng, "A new CPW-fed broad-band circularly polarized printed monopole antenna for UWB application," *Microw. Opt. Technol. Lett.*, vol. 60, no. 2, pp. 364–369, Feb. 2018.

[8] R. Q. Lee and K. Chun, "Compact miniaturized antenna for 210 MHz RFID," NASA Glenn Res. Center, Cleveland, OH, USA, Tech. Rep. NASA/TM–2002-211304, 2008, pp. 18–21.

[9] A. Loutridis, M. John, and M. J. Ammann, "Folded meander line antenna for wireless M-bus in the VHF and UHF bands," *Electron. Lett.*, vol. 51, no. 15, pp. 1138–1140, Jul. 2015.

[10] Y. Zhang and I. Glover, "Design of an ultrawideband VHF/UHF antenna for partial discharge detection," in *Proc. IEEE Int. Conf. Signal Process., Commun. Comput. (ICSPCC)*, Aug. 2014, pp. 487–490.

[11] Y. Qiang, W. Wang, and Y. Yao, "A printed ultra-wideband antenna with C-shaped ground plane for pattern stability," in *Proc. IEEE Int. Conf. Microw. Millim. Wave Technol. (ICMMT)*, vol. 2, Jun. 2016, pp. 749–751.

[12] T. Kim, Y. Kim, T. Yoo, and J. Yook, "Wideband planar monopole antenna for digital TV reception and UHF band communications," *IET Microw., Antennas Propag.*, vol. 12, no. 13, pp. 2041–2045, Oct. 2018.

[13] M. J. Ammann and M. John, "Optimum design of the printed strip monopole," *IEEE Antennas Propag. Mag.*, vol. 47, no. 6, pp. 59–61, Dec. 2005.

[14] L. Kai-Fong, "Microstrip patch antennas—Basic properties and some recent advances," *J. Atmos. Terr. Phys.*, vol. 51, nos. 9–10, pp. 811–818, Sep. 1989.

[15] R. Q. Lee, K. F. Lee, and J. Bobinchak, "Characteristics of a two-layer electromagnetically coupled rectangular patch antennas," *Electron. Lett.*, vol. 23, no. 20, pp. 1070–1072, 1987.

[16] R. B. Waterhouse, *Microstrip Patch Antennas: A Designer's Guide*. Boston: MA, USA: Kluwer, 2003.

[17] Jafri, Ely, and Vahala, "Graphical and statistical analysis of airplane passenger cabin RF coupling paths to avionics," in *Proc. 22nd Digit. Avionics Syst. Conf. (DASC)*, vol. 2, 2003, pp. 1–13.

[18] M. Randall, "Polarization and frequency diverse radar system for complete polarimetric characterization of scatterers with increased scanning speed," U.S. Patent 7 355 546 B2, Apr. 8, 2008.

[19] K. L. Chung, Y. Li, and C. Zhang, "Broadband artistic antenna array composed of circularly-polarized wang-shaped patch elements," *AEU-Int. J. Electron. Commun.*, vol. 74, pp. 116–122, Apr. 2017.

[20] K. L. Chung, X. Yan, Y. Li, and Y. Li, "A jia-shaped artistic patch antenna for dual-band circular polarization," *AEU-Int. J. Electron. Commun.*, vol. 120, Jun. 2020, Art. no. 153207.

[21] R. R. Ramirez and F. De Flaviis, "A mutual coupling study of linear and circular polarized microstrip antennas for diversity wireless systems," *IEEE Trans. Antennas Propag.*, vol. 51, no. 2, pp. 238–248, Feb. 2003.

[22] Nasimuddin, Z. Ning Chen, and X. Qing, "Dual-band circularly polarized *S*-shaped slotted patch antenna with a small frequency-ratio," *IEEE Trans. Antennas Propag.*, vol. 58, no. 6, pp. 2112–2115, Jun. 2010.

[23] K. L. Chung and S. Kharkovsky, "Mutual coupling reduction and gain enhancement using angular offset elements in circularly polarized patch array," *IEEE Antennas Wireless Propag. Lett.*, vol. 12, pp. 1122–1124, 2013.

[24] J. Li, M. Parlak, H. Mukai, M. Matsuo, and J. F. Buckwalter, "A reconfigurable 50-Mb/s-1 Gb/s pulse compression radar signal processor with offset calibration in 90-nm CMOS," *IEEE Trans. Microw. Theory Techn.*, vol. 63, no. 1, pp. 266–278, Dec. 2014.

[25] H. Yang, Y. Fan, and X. Liu, "A compact dual-band stacked patch antenna with dual circular polarizations for BeiDou navigation satellite systems," *IEEE Antennas Wireless Propag. Lett.*, vol. 18, no. 7, pp. 1472–1476, Jul. 2019.

[26] E. Torlaschi and A. R. Holt, "A comparison of different polarization schemes for the radar sensing of precipitation," *Radio Sci.*, vol. 33, no. 5, pp. 1335–1352, Sep. 1998.

[27] J. Calusdian, "Radiation patterns of antennas installed on aircraft," Naval Postgraduate School, Monterey, CA, USA, Tech. Rep., 1998. [Online]. Available: http://hdl.handle.net/10945/32613

[28] J. Huang, "A technique for an array to generate circular polarization with linearly polarized elements," *IEEE Trans. Antennas Propag.*, vol. 34, no. 9, pp. 1113–1124, Sep. 1986.

[29] J. L. Masa-Campos and F. Gonzalez-Fernandez, "Dual linear/circular polarized plannar antenna with low profile double-layer polarizer of 45° tilted metallic strips for wimax applications," *Prog. Electromagn. Res.*, vol. 98, pp. 221–231, 2009.

[30] W. H. Harman, J. D. Welch, and M. L. Wood, "Traffic alert and collision avoidance system (TCAS) surveillance performance in helicopters," Lincoln Lab., Massachusetts Inst. Technol., Lexington, MA, USA, Project Rep. ATC-135, 1987.

[31] D. De and P. K. Sahu, "An investigation on end-fire radiation from linearly polarized microstrip antenna for airborne systems," *Prog. Electromagn. Res. M*, vol. 59, pp. 9–24, Jul. 2017.

[32] D. De and P. K. Sahu, "Design and development of a unit element planar folded dipole end-fired antenna for aircraft collision avoidance system," *Prog. Electromagn. Res. C*, vol. 82, pp. 171–183, Mar. 2018.

[33] D. De and P. K. Sahu, "A novel approach towards the designing of an antenna for aircraft collision avoidance system," *AEU-Int. J. Electron. Commun.*, vol. 71, pp. 53–71, Jan. 2017.

[34] D. De and P. K. Sahu, "Design and development of a multi-feed end-fired microstrip antenna for TCAs airborne system," *Prog. Electromagn. Res. C*, vol. 78, pp. 69–81, Aug. 2017.

[35] L. Akhoondzadeh-Asl, J. J. Laurin, and A. Mirkamali, "A novel low-profile monopole antenna with beam switching capabilities," *IEEE Trans. Antennas Propag.*, vol. 62, no. 3, pp. 1212–1220, Mar. 2014.

[36] D. De and N. Chattoraj, "RF MEMS TCAS patch antenna," in *Proc. Int. Conf. Commun. Signal Process.*, Apr. 2014, pp. 1285–1292.

[37] M. S. A. Mohamed and A. M. M. A. Allam, "Design and implementation of a directional antenna for a traffic alert and collision avoidance system (TCAS)," in *Proc. 18th Medit. Microw. Symp. (MMS)*, Oct. 2018, pp. 79–82.

[38] K. Lee, R. Acosta, and R. Lee, "Microstrip antenna array with parasitic elements," in *Proc. Antennas Propag. Soc. Int. Symp.*, 1987, no. 1, pp. 794–797.

[39] S. A. R. Parizi, "Bandwidth enhancement techniques," in *Microstrip Antennas: Trends in Research on*, vol. 1. 2017, doi: 10.5772/intechopen.70173.

[40] R. K. Gupta and J. Mukherjee, "Low cost efficient high gain antenna using array of parasitic patches on a superstrate layer," *Microw. Opt. Technol. Lett.*, vol. 51, no. 3, pp. 733–739, Mar. 2009.

[41] R. K. Gupta and J. Mukherjee, "Efficient high gain with low sidelobe level antenna structures using circular array of square parasitic patches on a superstrate layer," *Microw. Opt. Technol. Lett.*, vol. 52, no. 12, pp. 2812–2817, Dec. 2010.

[42] Y. Gao, R. Ma, Y. Wang, Q. Zhang, and C. Parini, "Stacked patch antenna with dual-polarization and low mutual coupling for massive MIMO," *IEEE Trans. Antennas Propag.*, vol. 64, no. 10, pp. 4544–4549, Oct. 2016.

[43] Z. Yang, K. C. Browning, and K. F. Warnick, "High-efficiency stacked shorted annular patch antenna feed for ku-band satellite communications," *IEEE Trans. Antennas Propag.*, vol. 64, no. 6, pp. 2568–2572, Jun. 2016.

[44] H. Yang and N. Alexopoulos, "Gain enhancement methods for printed circuit antennas through multiple superstrates," *IEEE Trans. Antennas Propag.*, vol. 35, no. 7, pp. 860–863, Jul. 1987.

[45] R. Q. Lee and K.-F. Lee, "Experimental study of the two-layer electromagnetically coupled rectangular patch antenna," *IEEE Trans. Antennas Propag.*, vol. 38, no. 8, pp. 1298–1302, 1990.

[46] A. Sabban, "A new broadband stacked two-layer microstrip antenna," in *Proc. Antennas Propag. Soc. Int. Symp.*, 1983, pp. 63–66.

[47] C. Chen, A. Tulintseff, and R. Sorbello, "Broadband two-layer microstrip antenna," in *Proc. Antennas Propag. Soc. Int. Symp.*, vol. 1, 1984, pp. 251–254.

[48] P. S. Bhatnagar, J. P. Daniel, K. Mahdjoubi, and C. Terret, "Experimental study on stacked triangular microstrip antennas," *Electron. Lett.*, vol. 22, no. 16, pp. 864–865, Jul. 1986.

[49] J. Dahele, S. Tung, and K. Lee, "Normal and inverted configurations of the broadband electromagnetic-coupled microstrip antenna," in *Proc. Antennas Propag. Soc. Int. Symp.*, 1986, pp. 841–844.

[50] N. M. Cavallaro, J. F. Toth, and C. J. Alexander, "Microstrip antenna with parasitic elements," U.S. Patent 5 008 681 A, Apr. 16, 1991.

[51] S. Baudha, S. Gupta, and M. V. Yadav, "Parasitic rectangular patch antenna with variable shape ground plane for satellite and defence communication," in *Proc. URSI AP-RASC*, Mar. 2019, pp. 9–12.

[52] R. Q. Lee, T. Talty, and K. F. Lee, "Circular polarisation characteristics of stacked microstrip antennas," *Electron. Lett.*, vol. 26, no. 25, pp. 1021–1022, 1990.

[53] D. K. Cheng, "Gain optimization for Yagi-Uda arrays," *IEEE Antennas Propag. Mag.*, vol. 33, no. 3, pp. 42–46, Jun. 1991.

[54] M. A. Alkanhal and A. F. Sheta, "A novel dual-band reconfigurable square-ring microstrip antenna," *Prog. Electromagn. Res. PIER*, vol. 70, pp. 337–349, 2007.

[55] S. I. Latif, L. Shafai, and C. Shafai, "Ohmic loss reduction and gain enhancement of microstrip antennas using laminated conductors," in *Proc. 13th Int. Symp. Antenna Technol. Appl. Electromagn. Can. Radio Sci. Meeting*, no. 5, Feb. 2009, pp. 1–4.

[56] S. I. Latif, L. Shafai, and C. Shafai, "Gain and efficiency enhancement of compact and miniaturised microstrip antennas using multi-layered laminated conductors," *IET Microw., Antennas Propag.*, vol. 5, no. 4, pp. 402–411, 2011.

[57] S. I. Latif, C. Shafai, and L. Shafai, "Reduction in ohmic loss of small microstrip antennas using multiple copper layers," in *Proc. IEEE Antennas Propag. Soc. Int. Symp.*, Jul. 2006, pp. 1625–1628.

[58] E. G. Turitsyna and S. Webb, "Antenna miniaturisation using open-ring microstrip geometries," *Electron. Lett.*, vol. 42, no. 9, pp. 40–41, 2006.

[59] S. Oh and Y. Kim, "A compact bandpass filter using microstrip slow-wave open-loop resonators with high impedance lines," *Microw. Opt. Technol. Lett.*, vol. 38, no. 3, pp. 185–187, Aug. 2003.

[60] S. I. Latif, L. Shafai, and C. Shafai, "An engineered conductor for gain and efficiency improvement of miniaturized microstrip antennas," *IEEE Antennas Propag. Mag.*, vol. 55, no. 2, pp. 77–90, Apr. 2013.

[61] B. Yildirim and B. A. Cetiner, "Enhanced gain patch antenna with a rectangular loop shaped parasitic radiator," *IEEE Antennas Wireless Propag. Lett.*, vol. 7, pp. 229–232, 2008.

[62] E. Nishiyama and M. Aikawa, "Wide-band and high-gain microstrip antenna with thick parasitic patch substrate," in *Proc. IEEE Antennas Propag. Soc. Symp.*, Jun. 2004, pp. 273–276.

[63] S. Assailly, C. Terret, and J. P. Daniel, "Some results on broad-band microstrip antenna with low cross polar and high gain," *IEEE Trans. Antennas Propag.*, vol. 39, no. 3, pp. 413–415, Mar. 1991.

[64] V. Devaraj, K. K. Ajayan, and M. R. Baiju, "An optimised stacked e-shaped patch antenna," in *Proc. 2nd Eur. Conf. Antennas Propag. (EuCAP)*, 2007, pp. 1–6.

[65] H. A. Ochoa and Y. Y. Wodeamanuel, "Simulation of a microstrip patch antenna for 2. 4 GHz applications with radiation pattern in the horizontal direction," *Int. J. Appl. Eng. Res.*, vol. 12, no. 2, pp. 161–171, 2017.

[66] E. Sandi, A. Diamah, M. W. Iqbal, and D. N. Fajriah, "Double layer parasitic radiator for S-Band antennas to increase gain and bandwidth performances," *J. Phys., Conf. Ser.*, vol. 1402, Dec. 2019, Art. no. 044030.

[67] S. Egashira and E. Nishiyama, "Stacked microstrip antenna with wide bandwidth and high gain," *IEEE Trans. Antennas Propag.*, vol. 44, no. 11, pp. 1533–1534, 1996.

[68] P. Tilanthe, P. C. Sharma, and T. K. Bandopadhyay, "Gain enhancement of circular microstrip antenna for personal communication systems," *Int. J. Eng. Technol.*, vol. 3, no. 2, pp. 175–178, 2011.

[69] J.-S. Kuo and G.-B. Hsieh, "Gain enhancement of a circularly polarized equilateral-triangular microstrip antenna with a slotted ground plane," *IEEE Trans. Antennas Propag.*, vol. 51, no. 7, pp. 1652–1656, Jul. 2003.

[70] T. Zhang, S.-Y. Yao, and Y. Wang, "Design of radiation-pattern-reconfigurable antenna with four beams," *IEEE Antennas Wireless Propag. Lett.*, vol. 14, pp. 183–186, 2015.

[71] R. Q. Lee and K. F. Lee, "Gain enhancement of microstrip antennas with overlaying parasitic directors," *Electron. Lett.*, vol. 24, no. 11, pp. 656–658, May 1988.

[72] H. Legay and L. Shafai, "New stacked microstrip antenna with large bandwidth and high gain," *IEE Proc.-Microw., Antennas Propag.*, vol. 141, no. 3, pp. 199–204, Jun. 1994.

[73] A. S. Mekki, M. N. Hamidon, A. Ismail, and A. R. H. Alhawari, "Gain enhancement of a microstrip patch antenna using a reflecting layer," *Int. J. Antennas Propag.*, vol. 2015, pp. 1–7, 2015.

[74] T. Hidayat, F. Y. Zulkifli, and E. T. Rahardjo, "Bandwidth and gain enhancement of proximity coupled microstrip antenna using side parasitic patch," in *Proc. Antenna, Microw., Electron. Telecommun. (ICRAMET)*, Mar. 2013, pp. 95–98.

[75] J. A. Ansari, P. Singh, N. P. Yadav, and B. R. Vishvakarma, "Analysis of shorting pin loaded half disk patch antenna for wideband operation," *Prog. Electromagn. Res. C*, vol. 6, pp. 179–192, 2009.

[76] T. Sabapathy, R. B. Ahmad, M. Jusoh, and M. R. Kamarudin, "The effect of shorting pin locations on the performance of a pattern reconfigurable yagi-uda patch antenna," in *Proc. 2nd Int. Conf. Electron. Design (ICED)*, Aug. 2014, pp. 533–536.

[77] J. Liu and Q. Xue, "Broadband long rectangular patch antenna with high gain and vertical polarization," *IEEE Trans. Antennas Propag.*, vol. 61, no. 2, pp. 539–546, Feb. 2013.

[78] A. M. M. Dahlan and M. R. Kamarudin, "Shorted microstrip patch antenna with parasitic element," *J. Electromagn. Waves Appl.*, vol. 24, nos. 2–3, pp. 327–339, Jan. 2010.

[79] A. M. M. Dahlan and M. R. Kamarudin, "Shorted patch antenna with parasitic elements," *J. Electromagn. Waves Appl.*, vol. 24, pp. 2653–2655, Dec. 2009.

[80] X. Zhang and L. Zhu, "Gain-enhanced patch antennas with loading of shorting pins," *IEEE Trans. Antennas Propag.*, vol. 64, no. 8, pp. 3310–3318, Aug. 2016.

[81] X. Zhang and L. Zhu, "Gain-enhanced patch antenna without enlarged size via loading of slot and shorting pins," *IEEE Trans. Antennas Propag.*, vol. 65, no. 11, pp. 5702–5709, Nov. 2017.

[82] X. Zhang and L. Zhu, "Patch antennas with loading of a pair of shorting pins toward flexible impedance matching and low cross polarization," *IEEE Trans. Antennas Propag.*, vol. 64, no. 4, pp. 1226–1233, Apr. 2016.

[83] X. Zhang, L. Zhu, N. Liu, and D. Xie, "Pin-loaded circularly-polarised patch antenna with sharpened gain roll-off rate and widened 3-dB axial ratio beamwidth," *IET Microw., Antennas Propag.*, vol. 12, no. 8, pp. 1247–1254, Jul. 2018.

[84] S. M. Rathod, R. N. Awale, K. P. Ray, and S. S. Kakatkar, "Directivity enhancement of a circular microstrip antenna with shorting post," *IETE J. Res.*, pp. 1–10, May 2019, doi: 10.1080/03772063.2019.1612285.

[85] L. Z. X. Zhang, "Pin-loaded circularly-polarized patch antenna with enhanced gain," *IET Microw., Antennas Propag.*, vol. 12, no. 8, pp. 58–60, 2018.

[86] J. Liu, Q. Xue, H. Wong, H. W. Lai, and Y. Long, "Design and analysis of a low-profile and broadband microstrip monopolar patch antenna," *IEEE Trans. Antennas Propag.*, vol. 61, no. 1, pp. 11–18, Jan. 2013.

[87] K. Wei, Z. Zhang, and Z. Feng, "New coplanar capacitively coupled feeding method for circularly polarized patch antenna," in *Proc. IEEE Int. Symp. Antennas Propag. (APSURSI)*, Jul. 2011, pp. 3099–3102.

[88] D. Jackson and N. Alexopoulos, "Gain enhancement methods for printed circuit antennas," *IEEE Trans. Antennas Propag.*, vol. 33, no. 9, pp. 976–987, Sep. 1985.

[89] Y. Ju Lee, J. Yeo, R. Mittra, and W. Sang Park, "Application of electromagnetic bandgap (EBG) superstrates with controllable defects for a class of patch antennas as spatial angular filters," *IEEE Trans. Antennas Propag.*, vol. 53, no. 1, pp. 224–235, Jan. 2005.

[90] A. Foroozesh and L. Shafai, "Investigation into the effects of the patch-type FSS superstrate on the high-gain cavity resonance antenna design," *IEEE Trans. Antennas Propag.*, vol. 58, no. 2, pp. 258–270, Feb. 2010.

[91] N. Alexopoulos and D. Jackson, "Fundamental superstrate (cover) effects on printed circuit antennas," *IEEE Trans. Antennas Propag.*, vol. 32, no. 8, pp. 807–816, Aug. 1984.

[92] D. Schaubert, F. Farrar, A. Sindoris, and S. Hayes, "Microstrip antennas with frequency agility and polarization diversity," *IEEE Trans. Antennas Propag.*, vol. 29, no. 1, pp. 118–123, Jan. 1981.

[93] F. Yang and Y. Rahmat-Samii, "Applications of electromagnetic band-gap (EBG) structures in microwave antenna designs," in *Proc. 3rd Int. Conf. Microw. Millim. Wave Technol. (ICMMT)*, Aug. 2002, pp. 528–531.

[94] M. N. Aktar, M. Shahin Uddin, M. R. Amin, and M. M. Ali, "Enhanced gain and bandwidth of patch antenna using EBG substrates," *Int. J. Wireless Mobile Netw.*, vol. 3, no. 1, pp. 62–69, Feb. 2011.

[95] R. V. Sravya and R. Kumari, "Gain enhancement of patch antenna using L-slotted mushroom EBG," in *Proc. Conf. Signal Process. Commun. Eng. Syst. (SPACES)*, Jan. 2018, pp. 37–40.

[96] R. Manikonda, R. Valluri, M. R. Prudhivi, and B. S. S. Rao, "Enhancement of gain and bandwidth using EBG structure for textile antenna," *Int. J. Appl. Eng. Res.*, vol. 13, no. 15, pp. 11974–11978, 2018.

[97] C. R. Simovski, P. de Maagt, and I. V. Melchakova, "High-impedance surfaces having stable resonance with respect to polarization and incidence angle," *IEEE Trans. Antennas Propag.*, vol. 53, no. 3, pp. 908–914, Mar. 2005.

[98] W. Cao, B. Zhang, A. Liu, T. Yu, D. Guo, and X. Pan, "Multi-frequency and dual-mode patch antenna based on electromagnetic band-gap (EBG) structure," *IEEE Trans. Antennas Propag.*, vol. 60, no. 12, pp. 6007–6012, Dec. 2012.

[99] C. J. Meagher and S. K. Sharma, "A wideband aperture-coupled microstrip patch antenna employing spaced dielectric cover for enhanced gain performance," *IEEE Trans. Antennas Propag.*, vol. 58, no. 9, pp. 2802–2810, Sep. 2010.

[100] S. C. Kitson, W. L. Barnes, and J. R. Sambles, "Full photonic band gap for surface modes in the visible," *Phys. Rev. Lett.*, vol. 77, no. 13, pp. 2670–2673, Sep. 1996.

[101] K. B. Chung and S. W. Hong, "Wavelength demultiplexers based on the superprism phenomena in photonic crystals wavelength demultiplexers based on the superprism phenomena in photonic crystals," *Appl. Phys. Lett.*, vol. 81, no. 9, pp. 1549–1551, 2002.

[102] C. C. Chang, Y. Qian, T. Itoh, and H. Ave, "Compact and applications of uniplanar compact photonic bandgap structures," *Prog. Electromagn. Res.*, vol. 41, pp. 211–235, 2003.

[103] L. Yang, M. Fan, F. Chen, J. She, and Z. Feng, "A novel compact electromagnetic-bandgap (EBG) structure and its applications for microwave circuits," *IEEE Trans. Microw. Theory Techn.*, vol. 53, no. 1, pp. 183–190, Jan. 2005.

[104] S. Kim, Y.-J. Ren, H. Lee, A. Rida, S. Nikolaou, and M. M. Tentzeris, "Monopole antenna with inkjet-printed EBG array on paper substrate for wearable applications," *IEEE Antennas Wireless Propag. Lett.*, vol. 11, pp. 663–666, 2012.

[105] S. R. Hm and T. S. Rukmini, "Design and analysis of patch antenna with EBG for gain enhancement," in *Proc. IEEE Appl. Electromagn. Conf. (AEMC)*, Dec. 2013, pp. 6–7.

[106] Y. Zhang, N.-N. Zhang, J.-J. Chen, S.-W. Lu, Y. Zhai, and J. Zhang, "Design and application of rectangular spiral EBG," in *Proc. 9th Int. Symp. Antennas, Propag. EM Theory*, Nov. 2010, pp. 693–696.

[107] M. Saari, M. Isa, R. J. Langley, and S. Khamas, "Antenna control using EBG," in *Proc. 5th Eur. Conf. Antennas Propag. (EUCAP)*, Jul. 2014, pp. 216–219.

[108] S. K. Menon, B. Lethakumary, C. K. Aanandan, K. Vasudevan, and P. Mohanan, "A novel EBG structured ground plane for microstrip antennas," in *Proc. IEEE Antennas Propag. Soc. Int. Symp.*, Jul. 2005, pp. 578–581.

[109] N. S. Raghava and A. De, "Photonic bandgap stacked rectangular microstrip antenna for road vehicle communication," *IEEE Antennas Wireless Propag. Lett.*, vol. 5, pp. 421–423, 2006.

[110] H. Boutayeb and T. A. Denidni, "Gain enhancement of a microstrip patch antenna using a cylindrical electromagnetic crystal substrate," *IEEE Trans. Antennas Propag.*, vol. 55, no. 11, pp. 3140–3145, Nov. 2007.

[111] G. Ruvio, M. J. Ammann, and X. Bao, "Radial EBG cell layout for GPS patch antennas," *Electron. Lett.*, vol. 45, no. 13, pp. 1–2, 2009.

[112] J. Wang and K. Xie, "A new photonic crystal patch antenna based on EBG structure," in *Proc. IEEE Int. Conf. Inf. Theory Inf. Secur.*, Dec. 2010, pp. 898–902.

[113] R. Gonzalo, P. De Maagt, and M. Sorolla, "Enhanced patch-antenna performance by suppressing surface waves using photonic-bandgap substrates," *IEEE Trans. Microw. Theory Techn.*, vol. 47, no. 11, pp. 2131–2138, 1999.

[114] Krishnananda, K. R. Avinash, and T. S. Rukmini, "Design and performance analysis of EBG antenna for wireless applications," in *Proc. IEEE Appl. Electromagn. Conf. (AEMC)*, no. 3, Dec. 2011, pp. 9–12.

[115] M. Kamaszuk, "Gain enhancement methods for microstrip patch antennas," in *Proc. 1st Eur. Conf. Antennas Propag.*, Nov. 2006, pp. 6–11.

[116] H. Xu, Y. Lv, X. Luo, and C. Du, "Method for identifying the surface wave frequency band-gap of EBG structures," *Microw. Opt. Technol. Lett.*, vol. 49, no. 11, pp. 2668–2672, 2007.

[117] F. Fereidoony, S. Chamaani, and S. A. Mirtaheri, "UWB monopole antenna with stable radiation pattern and low transient distortion," *IEEE Antennas Wireless Propag. Lett.*, vol. 10, pp. 302–305, 2011.

[118] N. Rao and D. Kumar V., "Gain enhancement of microstrip patch antenna for Wi-Fi applications," in *Proc. Loughborough Antennas Propag. Conf. (LAPC)*, Nov. 2014, pp. 312–315.

[119] Y. Liu, Y. Hao, and S. Gong, "Low-profile high-gain slot antenna with Fabry–Pérot cavity and mushroom-like electromagnetic band gap structures," *Electron. Lett.*, vol. 51, no. 4, pp. 305–306, Feb. 2015.

[120] S. K. Sharma and L. Shafai, "Enhanced performance of an aperture-coupled rectangular microstrip antenna on a simplified unipolar compact photonic band gap (UC-PBG) structure," in *Proc. IEEE Antennas Propag. Soc. Int. Symp. Dig. Held Conjunct, USNC/URSI Nat. Radio Sci. Meeting*, 2001, pp. 498–501.

[121] R. Coccioli, F.-R. Yang, K.-P. Ma, and T. Itoh, "Aperture-coupled patch antenna on UC-PBG substrate," *IEEE Trans. Microw. Theory Techn.*, vol. 47, no. 11, pp. 2123–2130, 1999.

[122] J. C. Iriarte, I. Ederra, R. Gonzalo, A. Gosh, J. Laurin, C. Caloz, Y. Brand, M. Gavrilovic, Y. Demers, and P. de Maagt, "EBG superstrate for gain enhancement of a circularly polarized patch antenna," in *Proc. IEEE Antennas Propag. Soc. Int. Symp.*, no. 1, Jul. 2006, pp. 2993–2996.

[123] L. Leger, T. Monediere, and B. Jecko, "Enhancement of gain and radiation bandwidth for a planar 1-D EBG antenna," *IEEE Microw. Wireless Compon. Lett.*, vol. 15, no. 9, pp. 573–575, Sep. 2005.

[124] H. Xu, Z. Zhao, Y. Lv, C. Du, and X. Luo, "Metamaterial superstrate and electromagnetic band-gap substrate for high directive antenna," *Int. J. Infr. Millim. Waves*, vol. 29, no. 5, pp. 493–498, May 2008.

[125] D. R. Smith, W. J. Padilla, D. C. Vier, S. C. Nemat-Nasser, and S. Schultz, "Composite medium with simultaneously negative permeability and permittivity," *Phys. Rev. Lett.*, vol. 84, no. 18, pp. 4184–4187, May 2000.

[126] J. B. Pendry, "Negative refraction makes a perfect lens," *Phys. Rev. Lett.*, vol. 85, no. 18, pp. 3966–3969, Oct. 2000.

[127] M. Labidi, R. Salhi, and F. Choubani, "A design of metamaterial multi-band bowtie antenna based on omega-shaped resonator," *Appl. Phys. A, Solids Surf.*, vol. 123, no. 5, pp. 1–6, May 2017.

[128] D. Kholodnyak, V. Turgaliev, and E. Zameshaeva, "Dual-band immittance inverters on dual-composite right/left-handed transmission line (D-CRLH TL)," in *Proc. German Microw. Conf.*, Mar. 2015, pp. 60–63.

[129] H. Nornikman, B. H. Ahmad, M. Z. A. Abdul Aziz, M. F. B. A. Malek, H. Imran, and A. R. Othman, "Study and simulation of an edge couple split ring resonator (EC-SRR) on truncated pyramidal microwave absorber," *Prog. Electromagn. Res.*, vol. 127, pp. 319–334, Mar. 2012.

[130] J. N. Gollub, O. Yurduseven, K. P. Trofatter, D. Arnitz, M. F. Imani, T. Sleasman, M. Boyarsky, A. Rose, A. Pedross-Engel, H. Odabasi, T. Zvolensky, G. Lipworth, D. Brady, D. L. Marks, M. S. Reynolds, and D. R. Smith, "Large metasurface aperture for millimeter wave computational imaging at the human-scale," *Sci. Rep.*, vol. 7, no. 1, pp. 1–9, May 2017.

[131] F. Qin, L. Ding, L. Zhang, F. Monticone, C. C. Chum, J. Deng, S. Mei, Y. Li, J. Teng, M. Hong, and S. Zhang, "Hybrid bilayer plasmonic metasurface efficiently manipulates visible light," *Sci. Adv.*, vol. 2, no. 1, pp. 1–9, Jan. 2016.

[132] P. Kaur, S. K. Dr Aggarwal, and D. A. De, "A survey of techniques used for performance enhancement of patch antenna using metamaterials," *IOSR J. Electron. Commun. Eng.*, vol. 10, no. 6, pp. 98–109, 2015.

[133] S. Chaimool, K. L. Chung, and P. Akkaraekthalin, "Simultaneous gain and bandwidths enhancement of a single-feed circularly polarized microstrip patch antenna using a metamaterial reflective surface," *Prog. Electromagn. Res. B*, vol. 22, pp. 23–37, 2010.

[134] A. K. Panda and A. Sahu, "An investigation of gain enhancement of microstrip antenna by using inhomogeneous triangular metamaterial," in *Proc. Int. Conf. Comput. Intell. Commun. Netw.*, Oct. 2011, pp. 154–157.

[135] H. A. Majid, M. K. A. Rahim, and T. Masri, "Microstrip antenna's gain enhancement using left-handed metamaterial structure," *Prog. Electromagn. Res. M*, vol. 8, pp. 235–247, 2009.

[136] E. Dogan, E. Unal, D. Kapusuz, M. Karaaslan, and C. Sabah, "Microstrip patch antenna covered with left handed metamaterial," *Appl. Comput. Electromagn. Soc. J.*, vol. 29, no. 2, pp. 178–183, 2014.

[137] M. Alibakhshi-Kenari, M. Naser-Moghadasi, R. A. Sadeghzadeh, B. S. Virdee, and E. Limiti, "New CRLH-based planar slotted antennas with helical inductors for wireless communication systems, RF-circuits and microwave devices at UHF–SHF bands," *Wireless Pers. Commun.*, vol. 92, no. 3, pp. 1029–1038, Feb. 2017.

[138] C. H. Ng, K. K. A. Devi, C. K. Chakrabarty, N. Din, and C. F. Kwong, "Gain enhancement of microstrip patch antenna using low loss negative refractive index metamaterial superstrate," *J. Telecommun. Electron. Comput. Eng. Summ.*, vol. 9, no. 1, pp. 95–99, 2013.

[139] S. Roy and U. Chakraborty, "Gain enhancement of a dual-band WLAN microstrip antenna loaded with diagonal pattern metamaterials," *IET Commun.*, vol. 12, no. 12, pp. 1448–1453, Jul. 2018.

[140] S. Roy and U. Chakraborty, "Metamaterial-embedded dual wideband microstrip antenna for 2.4 GHz WLAN and 8.2 GHz ITU band applications," *Waves Random Complex Media*, vol. 30, no. 2, pp. 193–207, Apr. 2020.

[141] F. J. Herraiz-Martinez, G. Zamora, F. Paredes, F. Martin, and J. Bonache, "Multiband printed monopole antennas loaded with OCSRRs for PANs and WLANs," *IEEE Antennas Wireless Propag. Lett.*, vol. 10, pp. 1528–1531, 2011.

[142] R. Sahoo and D. Vakula, "Gain enhancement of conformal wideband antenna with parasitic elements and low index metamaterial for WiMAX application," *AEU-Int. J. Electron. Commun.*, vol. 105, pp. 24–35, Jun. 2019.

[143] J. P. G. Jeyaraj and A. Swaminathan, "Angled split-ring artificial magnetic conductor for gain enhancement in microstrip patch antenna for wireless applications," *Wireless Pers. Commun.*, vol. 101, no. 3, pp. 1221–1232, Aug. 2018.

[144] R. Salhi, M. Labidi, M. A. Boujemaa, and F. Choubani, "Dual-band microstrip patch antenna based on metamaterial refractive surface," *Appl. Phys. A, Solids Surf.*, vol. 123, no. 6, pp. 1–10, Jun. 2017.

[145] R. Pandeeswari and S. Raghavan, "Microstrip antenna with complementary split ring resonator loaded ground plane for gain enhancement," *Microw. Opt. Technol. Lett.*, vol. 57, no. 2, pp. 292–296, Feb. 2015.

[146] A. Ghosh, T. Mandal, and S. Das, "Design of triple band slot-patch antenna with improved gain using triple band artificial magnetic conductor," *Radioengineering*, vol. 25, no. 3, pp. 442–448, Sep. 2016.

[147] A. Ghosh, V. Kumar, G. Sen, and S. Das, "Gain enhancement of triple-band patch antenna by using triple-band artificial magnetic conductor," *IET Microw., Antennas Propag.*, vol. 12, no. 8, pp. 1400–1406, 2018.

[148] T. N. Chang, "Gain enhancement for circularly polarizes microstrip patch antenna," *Prog. Electromagn. Res. B*, vol. 17, pp. 275–292, 2009.

[149] K. K. A. Devi, N. C. Hau, C. K. Chakrabarty, and N. Md. Din, "Enhancement of band width and gain by using 3×4 array of metamaterial based patch antenna for RF energy harvesting at GSM 1800," *Int. J. Eng. Res.*, vol. 3, no. 10, pp. 618–623, Oct. 2014.

[150] H. Attia, O. Siddiqui, L. Yousefi, and O. M. Ramahi, "Metamaterial for gain enhancement of printed antennas: Theory, measurements and optimization," in *Proc. Saudi Int. Electron., Commun. Photon. Conf. (SIECPC)*, Apr. 2011, pp. 1–6.

[151] Z.-B. Weng, N.-B. Wang, Y.-C. Jiao, and F.-S. Zhang, "A directive patch antenna with metamaterial structure," *Microw. Opt. Technol. Lett.*, vol. 49, no. 2, pp. 456–459, Feb. 2007.

[152] M. Saravanan and S. M. Umarani, "Gain enhancement of patch antenna integrated with metamaterial inspired superstrate," *J. Electr. Syst. Inf. Technol.*, vol. 5, no. 3, pp. 263–270, Dec. 2018.

[153] H. Attia, L. Yousefi, M. M. Bait-Suwailam, M. S. Boybay, and O. M. Ramahi, "Enhanced-gain microstrip antenna using engineered magnetic superstrates," *IEEE Antennas Wireless Propag. Lett.*, vol. 8, pp. 1198–1201, 2009.

[154] S. N. Burokur, A.-C. Lepage, S. Varault, X. Begaud, G.-P. Piau, and A. de Lustrac, "Low-profile metamaterial-based L-band antennas," *Appl. Phys. A, Solids Surf.*, vol. 122, no. 4, pp. 3–9, Apr. 2016.

[155] W. Yang, W. Che, and H. Wang, "High-gain design of a patch antenna using stub-loaded artificial magnetic conductor," *IEEE Antennas Wireless Propag. Lett.*, vol. 12, pp. 1172–1175, 2013.

[156] J. Joubert, J. C. Vardaxoglou, W. G. Whittow, and J. W. Odendaal, "CPW-fed cavity-backed slot radiator loaded with an AMC reflector," *IEEE Trans. Antennas Propag.*, vol. 60, no. 2, pp. 735–742, Feb. 2012.

[157] Y. Zhong, G. Yang, and L. Zhong, "Gain enhancement of bow-tie antenna using fractal wideband artificial magnetic conductor ground," *Electron. Lett.*, vol. 51, no. 4, pp. 315–317, Feb. 2015.

[158] P. Arnmanee and C. Phongcharoenpanich, "Improved microstrip antenna with HIS elements and FSS superstrate for 2.4 GHz band applications," *Int. J. Antennas Propag.*, vol. 2018, pp. 1–11, 2018.

[159] Q. Luo, H. Tian, Z. Huang, X. Wang, Z. Guo, and Y. Ji, "Unidirectional dual-band CPW-fed antenna loaded with an AMC reflector," *Int. J. Antennas Propag.*, vol. 2013, pp. 1–10, Oct. 2013.

[160] M. Ullah, M. Islam, and M. Faruque, "A near-zero refractive index meta-surface structure for antenna performance improvement," *Materials*, vol. 6, no. 11, pp. 5058–5068, Nov. 2013.

[161] N. Kushwaha and R. Kumar, "Design of a wideband high gain antenna using FSS for circularly polarized applications," *Int. J. Electron. Commun.*, vol. 70, no. 9, pp. 1–8, 2016.

[162] M. Islam, M. Ullah, M. Singh, and M. Faruque, "A new metasurface superstrate structure for antenna performance enhancement," *Materials*, vol. 6, no. 8, pp. 3226–3240, Jul. 2013.

[163] K. L. Chung and S. Chaimool, "Broadside gain and bandwidth enhancement of microstrip patch antenna using a MNZ-metasurface," *Microw. Opt. Technol. Lett.*, vol. 54, no. 2, pp. 529–532, Feb. 2012.

[164] D. Sievenpiper, L. Zhang, R. F. J. Broas, N. G. Alexopolous, and E. Yablonovitch, "High-impedance electromagnetic surfaces with a forbidden frequency band," *IEEE Trans. Microw. Theory Techn.*, vol. 47, no. 11, pp. 2059–2074, 1999.

[165] F. Yang and Y. Rahmat-Samii, "Microstrip antennas integrated with electromagnetic band-gap (EBG) structures: A low mutual coupling design for array applications," *IEEE Trans. Antennas Propag.*, vol. 51, no. 10, pp. 2936–2946, Oct. 2003.

[166] S. Enoch, G. Tayeb, P. Sabouroux, N. Guérin, and P. Vincent, "A metamaterial for directive emission," *Phys. Rev. Lett.*, vol. 89, no. 21, pp. 1–4, Nov. 2002.

[167] N. Bahari, M. F. Jamlos, and M. M. Isa, "Gain enhancement of microstrip patch antenna using artificial magnetic conductor," *Bull. Electr. Eng. Informat.*, vol. 8, no. 1, pp. 166–171, Mar. 2019.

[168] W. Yang, D. Chen, and W. Che, "High-efficiency high-isolation dual-orthogonally polarized patch antennas using nonperiodic RAMC structure," *IEEE Trans. Antennas Propag.*, vol. 65, no. 2, pp. 887–892, Feb. 2017.

[169] Y.-J. Zheng, J. Gao, X.-Y. Cao, S.-J. Li, and W.-Q. Li, "Wideband RCS reduction and gain enhancement microstrip antenna using chessboard configuration superstrate," *Microw. Opt. Technol. Lett.*, vol. 57, no. 7, pp. 1738–1741, Jul. 2015.

[170] G.-M. Yang, X. Xing, A. Daigle, O. Obi, M. Liu, J. Lou, S. Stoute, K. Naishadham, and N. X. Sun, "Planar annular ring antennas with multilayer self-biased NiCo-ferrite films loading," *IEEE Trans. Antennas Propag.*, vol. 58, no. 3, pp. 648–655, Mar. 2010.

M. PALLAVI (Graduate Student Member, IEEE) received the B.E. degree in instrumentation technology and the M.Tech. degree in information and communication systems from Visvesvaraya Technological University, Belgaum, India. She is currently pursuing the Ph.D. degree with the Department of Electronics and Communication Engineering, Manipal Institute of Technology, Manipal Academy of Higher Education, Manipal, India.

Her current research interests include feeding mechanism for antenna, linearly polarized microstrip antennas, microstrip antenna applications, and performance enhancement techniques for microstrip antennas. She is an Associate Member of IETE and ISTE.

PRAMOD KUMAR is currently working as an Associate Professor-Senior Scale with the Department of Electronics and Communication Engineering, Manipal Institute of Technology, Manipal Academy of Higher Education, Manipal. He is an Active Researcher in the field of microstrip antennas and wireless communication. He has published more than 25 articles in reputed peer-reviewed international journal and conferences. He is on the board of reviewers of journals like, *IET Electronics Letters*, *Wireless Personal Communication* (WPC), (Springer), and AEU-*International Journal of Electronics and Communications*.

TANWEER ALI (Senior Member, IEEE) is currently working as an Assistant Professor-Senior Scale with the Department of Electronics and Communication Engineering, Manipal Institute of Technology, Manipal Academy of Higher Education, Manipal. He is an Active Researcher in the field of microstrip antennas, wireless communication, and microwave Imaging. He has published more than 100 articles in reputed peer-reviewed international journal and conferences. He is an Associate Member of IETE India. He is on the board of reviewers of journals like the IEEE Transactions on Antennas and Propagation, IEEE Antennas and Wireless Propagation Letters, IEEE Access, *IET Microwaves, Antennas and Propagation*, *IET Electronics Letters*, *Wireless Personal Communication* (WPC), (Springer), AEU-*International Journal of Electronics and Communications*, *Microwave and Optical Technology Letters* (MOTL), (Wiley), *International Journal of Antennas and Propagation*, (Hindawi), *Advanced Electromagnetics*, *Progress in Electromagnetic Research* (PIER), *KSII Transactions of Engineering Science*, South Korea, *International Journal of Microwave and Wireless Technologies*, *Frequency*, *Radio engineering*, and so on.

SATISH B. SHENOY is currently working as a Professor with the Department of Aeronautical and Automobile Engineering, Manipal Institute of Technology (MIT), Manipal Academy of Higher Education, Manipal. He is on the Mentor Board of the Center for Excellence in Avionics and Navigation Systems, MIT, Manipal. He is an Active Researcher in the field CFD, FEM, and CAD. He has published more than 88 articles in reputed peer-reviewed journals. He is a Life Member of TSI. He is on the board of reviewers of journals like *Tribology International*, *Proceedings of the Institution of Mechanical Engineers, Part J: Journal of Engineering Tribology*, *Computer Methods in Biomechanics and Biomedical Engineering*, *Journal of the Brazilian Society of Mechanical Sciences and Engineering*, *Simulation Modelling Practice and Theory*, *Tribology Transactions*, *Industrial Lubrication and Tribology*, *Journal of Tribology*, *Polymer Testing*, *Acta Radiologica*, *Journal of Bionic Engineering*, *Journal of Marine Science and Application*, *Mechanics and Industry*, and *Polymer Composites*.

• • •